Seasonal and Flood-Induced Variations in Groundwater-Surface Water Exchange Dynamics in a Shallow Aquifer System: Amity Creek, MN

A Thesis
SUBMITTED TO THE FACULTY OF
UNIVERSITY OF MINNESOTA
BY

Jenny L. Jasperson

IN PARTIAL FULFILLMENT OF THE REQUIREMENTS
FOR THE DEGREE OF
MASTER OF SCIENCE

Karen Gran, Joe Magner

January 2016

ACKNOWLEDGEMENTS

This project would not have been possible without professors Dr. Karen Gran and Dr. Joe Magner. Joe Magner believed in my ability to take a lead role in this project and encouraged my professional and educational development throughout the process. Karen Gran was my lead supporter throughout the project. I am grateful for her encouragement, patience, scientific enthusiasm, and guidance.

I would like to thank the Minnesota Pollution Control Agency (MPCA) for providing primary funding and technical staff assistance. I am especially thankful for the support of Pat Carey in recognizing the value of this study in the MPCA's watershed-wide monitoring approach, specifically for the Lake Superior South major watershed. Andrew Streitz provided valuable technical assistance and guidance in the groundwater component of the study. Many other MPCA staff provided advice, field skills, knowledge, and professional and personal support and I am incredibly grateful.

I am also thankful for the technical guidance and instruction in hydrogeology provided by University of Minnesota Duluth (UMD) professors Dr. John Swenson and Dr. Howard Mooers. Former UMD graduate students, Emily Dunn, Molly Wick, Grant Neitzel, and Josh Allen provided humor and support that was most helpful during my course work.

Finally I would like to thank Jeff Jasperson for his overwhelming professional and personal support. He provided critical context to the biological significance of this study and recognized the study's value in the biological Stressor Identification approach for the Lake Superior South major watershed. I thank him personally along with my children for their patience during this time and for countless hours of enjoyment on North Shore of Lake Superior streams.

ABSTRACT

Excellent brook trout habitat can be found in segments of many streams on the North Shore of Lake Superior. Optimal riverine brook trout habitat includes clear, cold spring-fed water and studies have shown that areas of groundwater upwelling in streams tend to be more important than other site selection variables. Observations of historical brook trout and temperature data in the Amity Creek sub-watershed of Lake Superior South HUC-8 led us to hypothesize that reaches with healthy and stable brook trout communities are likely connected to groundwater storage, exchange, and upwelling.

Climate trend models for the Midwest predict future changes in temperature, annual precipitation, and storm event frequency for Northern Minnesota. Streams along the North Shore of Lake Superior are susceptible to increased temperatures and insufficient late summer to early winter flows due to climate change and the unique regional geology. Understanding groundwater-surface water hydrology interactions, watershed connectivity, and related flood-induced geomorphic and hydrologic changes is important because they relate to the overall stability and aquatic health of the stream and the biological communities that inhabit it.

The objectives of this study were to identify groundwater storage zones, upwelling zones, and seasonal variations; and assess how these relationships change as result of a major flood. A study reach on East Branch Amity Creek is incising through clay-rich glacial tills overlying bedrock and has avulsed multiple times in the past, stranding discrete remnant channels cut into till. A 500-year storm hit Duluth, MN, USA on June 19-20th 2012, producing 8-inches of rain in a 24-hour duration which resulted in

flash flooding across the region. Pre-flood and post-flood groundwater and surface water level data were collected through a series of piezometers with pressure transducers and an in-channel stream gage. Stable isotope analyses of Deuterium and Oxygen-18 were conducted on water samples with varying temporal and spatial variability to provide information on watershed and reach-scale source hydrology and evaluate flood-induced changes.

Results show groundwater upwelling variability within the greater watershed and identify two discrete groundwater storage zones within a smaller study reach. Pre- and post-flood analyses show a correlation between incision in main stem and remnant channels and a lowered water table, following the flood. Isotope analysis indicates a temporary post-flood change in subsurface source water. Because much of the greater North Shore of Lake Superior has the same geology as the study area, the results of this study may provide insight to hydrology studies of other North Shore streams.

TABLE OF CONTENTS

LIST OF TABLES

LIST OF FIGURES

INTRODUCTION

The interaction of groundwater and surface water has been studied for decades in a wide variety of settings. The exchange relationship can be complex and is influenced by many factors. These include topography, geology, streambed permeability, channel shape, hydraulic gradient, and the stream flow regime. In addition, the exchange interactions are often dynamic, varying spatially and temporally. The exchange relationship can vary longitudinally within a stream system, with some reaches gaining from groundwater and other reaches losing to groundwater (Winter et al., 1998). Within a given reach and throughout the greater system, the size of the hyporheic zone, the area of exchange beneath and adjacent to the stream channel, and related bank storage volume and fluxes vary with changes in the environmental conditions such as stream water level fluctuations and river bank conditions. (Siergieiev et al., 2015).

The characteristics of the hyporheic zone can markedly influence stream temperatures, water chemistry, the hydrological regime, and coldwater fisheries. Optimal riverine brook trout habitat includes clear, cold spring-fed water in addition to slow-moving deep pockets of water. There is a definite positive relationship between quality of trout habitat and adequate late summer and early winter baseflows (Raleigh, 1982). Studies have shown that areas of groundwater upwelling in streams are highly preferred for spawning and tend to be more important than other site selection variables such as substrate size (Webster and Eiriksdottier, 1976; Carline and Brynildson, 1977). Baxter and Hauer (2000) state that maintenance of spawning habitat for bull trout, a coldwater

sensitive species, require consideration of groundwater-surface water exchange within a geomorphic context and include reach, segment, and watershed-scale analysis. Their study found that reaches influenced by groundwater discharge provide stable thermal and flow regimes that influence spawning and survival.

Excellent brook trout habitat can be found in segments of many Lake Superior South (LSS) streams. Lake Superior South Hydrologic Unit Code (HUC)-8 watershed is a long and narrow-shaped watershed in northeast Minnesota that drains individual streams into the southwest corner of Lake Superior in a series of parallel stream network systems. The streams in this drainage are generally small in size and derive from headwater bogs and wetlands. Soils can be shallow to deep and range from denser clay loam and clay glacial till to more permeable organics and alluvium (MPCA, 2014). In general, groundwater storage is shallow due to thick clay soils, shallow depth to bedrock, and a lack of deep aquifers. Stream channels in the upper and middle portions of the parallel sub-watersheds vary in gradient and then descend with a much greater slope toward Lake Superior in their lower portions.

The stream hydrology in the majority of the watershed is flashy due to shallow depth to bedrock, slower infiltration rates in the clay till, and areas of steep gradient. Extreme low mid-to-late summer baseflows are common which can increase stream temperatures and limit dissolved oxygen and physical habitat, stranding brook trout in individual, shallow to moderate-depth pools. This is especially common in losing reaches. In addition, high surface runoff rates on clay soils and bedrock during snowmelt

and rain events result in warm, fast, turbulent, and turbid in-channel flows which cause temporary or more long-term unsuitable habitat conditions for brook trout.

The abundance of brook trout and influencing variables such as stream temperature, physical habitat, and groundwater inputs to the stream are not uniform throughout the watersheds. Data collection through various efforts in the Lake Superior South sub-watersheds has shown that some stream reaches have exceptional fish and invertebrate communities, whereas others have moderate to poor communities (Axler et al., 2013; MNDNR, 2002; MPCA, 2014). The communities are more stable in some reaches than others which indicate the quality of habitat is less vulnerable to seasonal climatic change (Axler et al., 2013). Water chemistry is also more stable in some reaches than others. Median late summer stream temperature and dissolved oxygen values vary among streams and reaches. The magnitude of diurnal oscillations can also vary, showing that some areas are less influenced by daily changes in air temperature.

Healthier brook trout habitat typically is found in the headwaters and middle sections of the streams that make up the watershed. The lower stream segments are limited by temperatures and fines in the water (MPCA, 2014). The upper watersheds tend to have more potential for surficial and subsurface water storage due to lesser gradient, greater depth to bedrock, and the presence of wetlands, depressions, and swales. These areas of storage help buffer flows by holding back water during high-volume flow events and recharging the stream during periods of lower flow.

Habitat and physical stream conditions in less stable or developed areas of the watershed are dynamic. Shifting of the bed between both aggradation and incision

commonly occur multiple times within a season. Mass slumping of clay banks during snowmelt and summer rain events is also common. During the course of this study, a 500- year flood event occurred in the Duluth, MN, USA, area and affected the majority of the Lake Superior South sub-watersheds. A varied degree of geomorphic response, from catastrophic to negligible damage, occurred in area streams. This rare occurrence provided us the opportunity to evaluate groundwater composition and elevation response to geomorphic changes that occurred in the stream channel and floodplain.

Study Objectives

The objectives of this study were to examine groundwater-surface water interactions and characterize the water budget within a given reach and within the greater watershed of a Lake Superior South stream. Amity Creek, a coldwater trout stream in Duluth, MN, was chosen. Observations of historical brook trout and temperature data in the Amity Creek watershed led us to hypothesize that reaches with healthy and stable brook trout communities in the watershed are likely connected to groundwater storage, exchange, and upwelling. Based on the geology, the primary sources of recharge are *(i)* shallow subsurface flow from infiltrated and pooled water in depressions in the floodplain and/or *(ii)* more dominant natural springs driven by wetlands, topography, and/or lenses of alluvium or glacial outwash. The specific research objectives were to *(i)* identify locations of groundwater – surface water exchange including groundwater storage zones, upwelling zones, and seasonal variations and (ii) assess how these relationships change as result of a major flood. To do this, we monitored a reach, both

groundwater and surface water, prior to and after the 2012 flood using water level data and isotopic signatures in addition to isotopic characterization of the greater watershed.

Climate trend models for the Midwest predict future changes in temperature, annual precipitation, and storm event frequency for Northern Minnesota. Streams along the North Shore of Lake Superior are susceptible to increased temperatures and insufficient late summer to early winter flows due to climate change and the unique regional geology. Understanding groundwater-surface water hydrology interactions, watershed connectivity, and related flood-induced geomorphic and hydrologic changes is important because they relate to the overall stability and aquatic health of the stream and the biological communities that inhabit it. The findings from the Amity Creek watershed will help shape the understanding of the groundwater - surface water exchange dynamics in other streams of the Lake Superior South watershed. Identifying stream reaches with greater groundwater inputs may also lay the framework for preservation activities in the watershed including land preservation, habitat improvement projects, and zoning and development.

STUDY AREA

The Amity Creek watershed (Fig. 1), a 16 mi^2 drainage within the LSS basin and located on the eastern edge of Duluth, MN, is a primarily-forested watershed with some rural development dispersed throughout and urban development present in the lowest reaches. Flow pattern within the Amity system is dendritic and primarily oriented from northwest to southeast. Stream channel elevations range from 1412 feet above mean sea

level (AMSL) in the headwaters to 625 feet at the stream's confluence with the Lester River. The Lester River enters Lake Superior at an elevation of 600 feet, just 0.25 miles downstream from the Amity Creek confluence. A main tributary, East Branch Amity Creek, enters the system from the north and east at 3.3 miles upstream of the Amity-Lester confluence.

The geologic history that helped shape the watershed consists of glacial activity over ancient lava flows. The underlying bedrock, formed from basalt lava flows and igneous intrusions, is a product of a Mid-Continental Rift that occurred 1.1 billion years ago (Sims & Morey, 1972). Bedrock is at or near the land surface in the lower watershed where Quaternary soils are thin or have been eroded away completely. A thick diabase layer, the Northland sill, is present at an elevation of 950 feet AMSL (Fig. 1) and appears as a prominent scarp in the landscape (Green, 1972). Amity Creek is bounded to the south by the sill in the mid-watershed as it flows in a southwest to northeast direction. The stream is re-directed 90 degrees south where it cross-cuts the sill and then descends down a steep bedrock escarpment towards Lake Superior.

Thicker Quaternary deposits in the form of supraglacial drift and lower stream channel gradients (Figs. 1 & 2) are present in the upper watershed (Fitzpatrick et al., 2006). East Branch Amity Creek watershed is primarily formed in these deposits with shallower depth to bedrock in the lower reaches of the drainage. The change from thicker to thinner soils over bedrock coincides with a break in the stream channel at approximately 1250 feet AMSL and corresponds to an end moraine. The landscape upstream of the transition is characterized by thicker soils, glacial lake plains, and slower

hydrological response buffered by wetland abundance and stream-floodplain connection. Wetlands and lowered stream gradients within a widened valley are located downstream of the moraine. At 1190 feet AMSL, the valley narrows resulting in steepened stream gradients and increased entrenchment. Glacial Lake Duluth shoreline features are mapped at stream and upland elevations of 1040 and 1082 feet AMSL respectively (Breckenridge, 2013). Discrete deltaic features are observed upstream of the shoreline and downstream of the 1190 feet AMSL valley constriction.

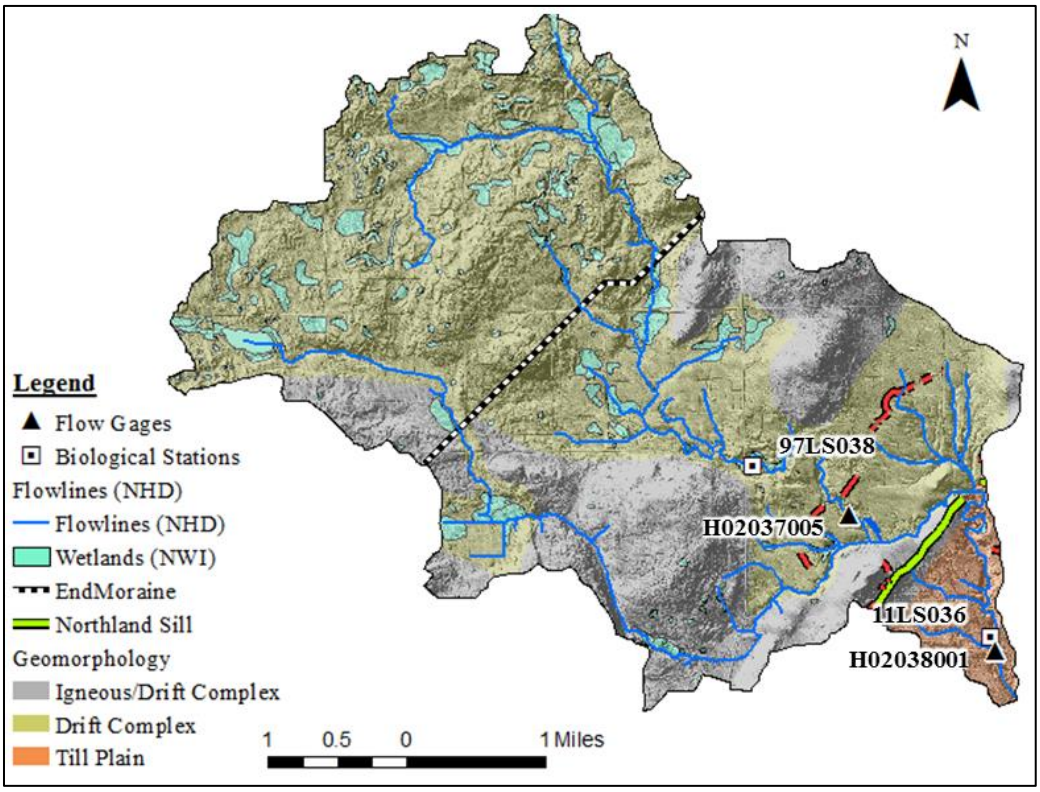

Figure 1. Amity Creek watershed (Duluth, MN) map showing geomorphology (University of Minnesota-Duluth Geology Department, 1997), flowlines (from the United States Geological Survey's National Hydrography Dataset (NHD)) , wetlands (from the National Wetlands Inventory (NWI)), and MPCA flow gages and biological stations. Flow gage H02038001 is located at Lat: 46.84N, Long: 92.01W.

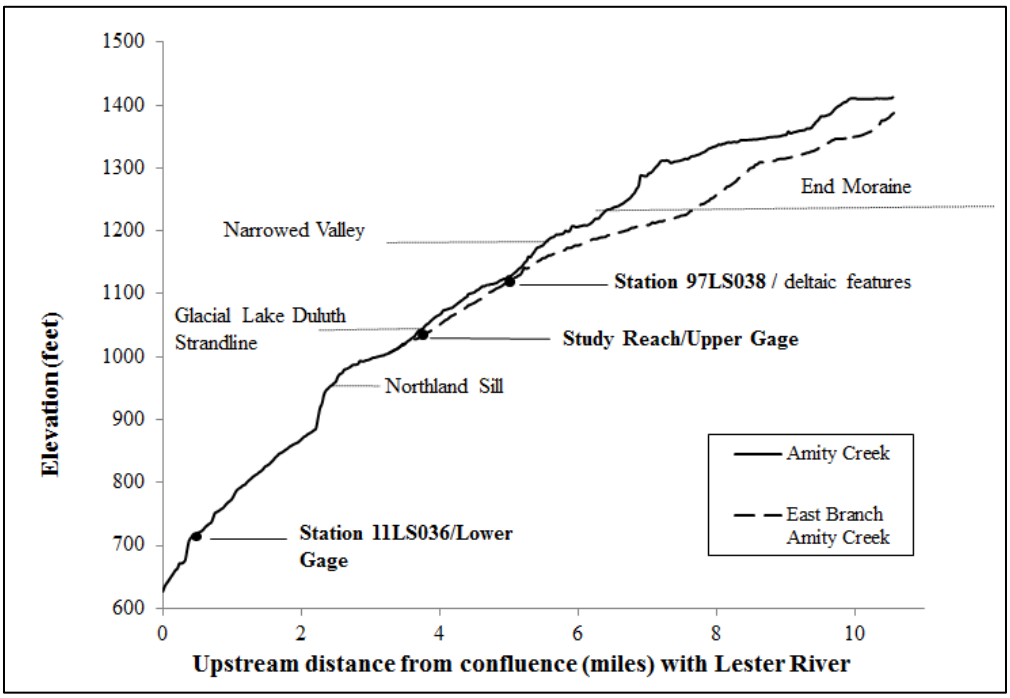

Figure 2. Longitudinal profile of Amity Creek and East Branch Amity Creek (Duluth, MN) showing dominant channel-forming geologic features and monitoring stations. The lower gage H02038001 and biological station 11LS036 are located at Lat: 46.84N, Long: 92.01W

In 2011, a watershed-wide monitoring approach was implemented in the LSS watershed by the Minnesota Pollution Control Agency (MPCA). As part of this effort, indices of biological integrity (IBI) were calculated for fish and macroinvertebrate communities based on sample data collection. Two biological stations (Figs. 1 & 2) were monitored in the Amity Creek watershed: station 11LS036 on a lower bedrock reach of Amity Creek and station 97LS038 located on East Branch Amity Creek in the vicinity of deltaic sediment features and upstream of the glacial lake shoreline. Brook trout densities for the Amity Creek and East Branch Amity Creek stations are respectively 0.008 and 0.348 brook trout per meter. The respective percentiles in context to all reportable coldwater streams (n=95) in the Arrowhead region of northeast Minnesota for years

2009-2014, are 15th and 95th (MPCA, 2015). Continuous stream temperature data were collected at both biological stations, June through August, 2011. Temperatures at the main stem site were in the primary growth range (8-20 ºC) 70% of the time indicating fair thermal conditions. Stream temperatures at the East Branch site were in the primary growth range 96% of the time indicating good thermal conditions.

MPCA flow gage stations, reporting 15 minute interval stream stage, flow, and temperature data were operating on Amity Creek (H02038001) and East Branch Amity Creek (H02037005) during a sub-period of the study timeframe (2010-2013). Reportable data were available for the Amity Creek gage, in operation from 2002 to present, for study years 2010-2012. The East Branch Amity gage was installed in 2011, recording a partial record (2011-2012) of the study time period. Provisional gage data for year 2013 were not reported out prior to completion of this study.

CLIMATE YEARS

Weather in Duluth, MN, moderated by Lake Superior, is characterized by short warm summers and long cold winters. Temperatures along the shoreline can be much cooler in the summer and warmer in the winter than inland temperatures due to lake effect. Normal daily maximum air temperatures range from 18 º F in January to 76 º F in July. Wind speed, atmospheric vapor, and pressure belts can also be influenced by the lake, resulting in localized and enhanced storm systems. Moisture rising from the lake during winter months creates localized snow storms in the highlands that contribute to making this the snowiest region in the state of Minnesota with normal mean annual

snowfall totals of 86 inches (GGWS, 2015). Precipitation is influenced by both Arctic and Gulf air masses. Mean annual precipitation is 31 inches, most of which is received May through October. Most of the precipitation is returned to the atmosphere through evapotranspiration. Mean annual runoff rates of 10-12 inches are the highest in Minnesota (Lorenz et al., 2010) and mean annual evaporation is 29 inches (Dadaser-Celik and Stefan, 2008).

National Weather Service data reported through the Minnesota Climatology Working Group (MCWG, 2010-2013) and MPCA stream gage data (MPCA, 2010-2012) were used to summarize weather and stream response conditions for the study period. Year 2010 was a warmer than average year with an early snowmelt and multiple runoff events in May and June. The stream over-topped its banks with a 3-inch rain event in late October. Year 2011 experienced a 2.5 inch runoff event in June and a 100-year rain event in early August. Despite these large storms, the U.S. Drought Monitor declared a moderate to severe drought in late summer and autumn. Year 2012 was characterized by below average snowpack, a 500-year flood event in June, and severe drought conditions by September. Additional substantial flow events in year 2012 included a 2 inch runoff event on saturated soils in April and a 3-inch rain event in May. Year 2013 began with historic high snowfall records in April. Above bankfull conditions were recorded during spring snowmelt and again during a May 21st rain event. No moderate to major rain events occurred after June in year 2013.

FIELD AND LABORATORY METHODS

Our study investigated surface water – groundwater interactions at both watershed and reach-scales. Drainage-scale analysis of water budget characterization including evaporative losses and groundwater upwelling zones was focused on the greater Amity Creek drainage. A more detailed reach-scale analysis of exchange was conducted on East Branch Amity Creek, just upstream of the confluence with Amity Creek (Fig. 3). Isotopic tracers of oxygen and hydrogen in combination with water level data were used to define groundwater storage zones and flow interactions between zones in the adjacent floodplain of the study reach, capturing seasonal variability. Groundwater levels and isotopic composition prior to and after the flood were compared.

Watershed-Wide Isotope Sample Collection

Samples were collected across the Amity Creek watershed (Fig. 3) in years 2010-2012 with most intense sampling occurring in 2012 in addition to one sample collected in July 2014. Stream surface water from nine locations across the watershed was sampled during snowmelt, baseflow, and rain-event conditions. Samples were collected at mid-depth in the stream channel, and faster moving water was preferred over slower or stagnant waters where possible. Sample site SW13 was located at biological station 97LS038. Precipitation samples were collected monthly in 2012 in the Lakeside neighborhood of Duluth (Lat: 46.83N, Long: 92.03W), within a mile of the watershed boundary. Additional snowpack samples were collected from sites adjacent to surface water locations throughout the watershed during April 2011 and March 2012. Water

samples were collected in 125 mL to 250 mL high-density polyethylene (HDPE) bottles with minimal headspace. Snow was collected in 1L HDPE bottles and then transferred to smaller bottles after melting.

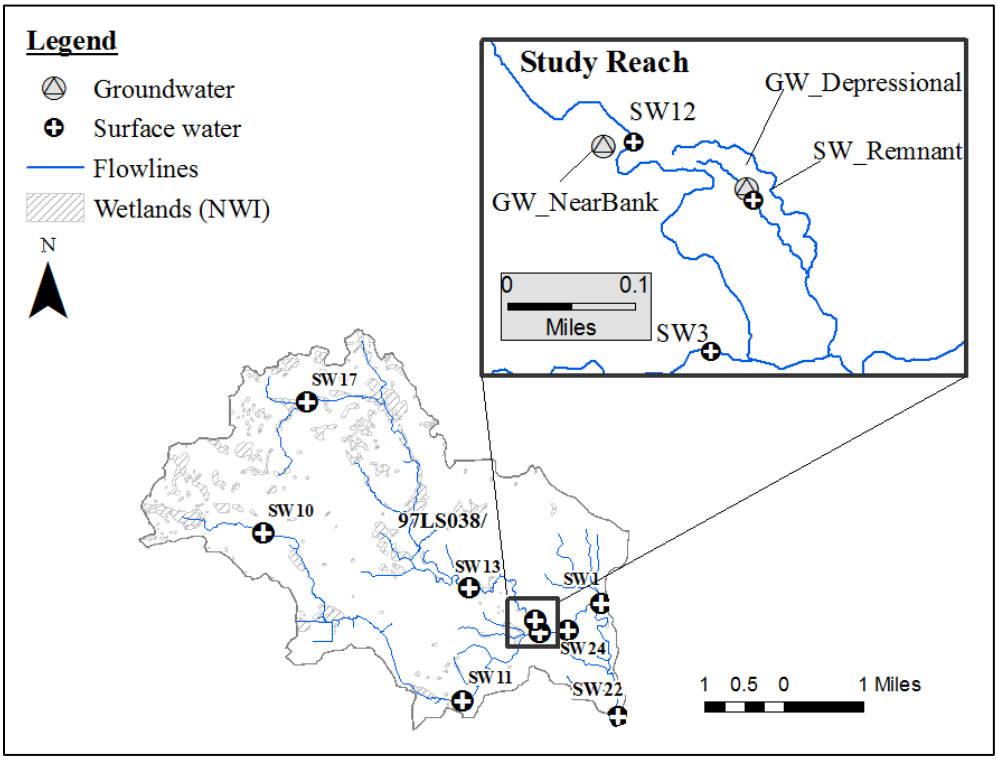

Figure 3. Map of surface water and groundwater isotope sample locations, flowlines from the National Hydrography Dataset (watershed-scale) and delineated using LiDAR imagery (study reach), and wetlands from the National Wetlands Inventory (NWI). Groundwater sample locations consist of near-bank piezometers and depressional piezometers. Insert map shows location of the study reach.

Isotope Laboratory Analysis

Samples were submitted to the Biometeorology Lab at the University of Minnesota for analysis using a DLT-100 liquid water isotope analyzer. Results were reported in delta (δ) notation in units of ‰ relative to Vienna Standard Mean Ocean Water (VSMOW), [$\delta = (R_{sample}/R_{VSMOW} - 1)$ X 1000], where R_{sample} is the isotope ratio

($^{18}O/^{16}O$, $^{2}H/^{1}H$) of the sample and R_{VSMOW} is the isotope ratio of the standard (Schultz et al., 2011). Samples (n = 7) with analytical uncertainties greater than 2 ‰ for $\delta^{2}H$ and 0.25 ‰ for $\delta^{18}O$ were excluded from the analysis including and in addition to all 2013 samples due to analyzer issues. Lab results for samples included in the analysis can be found in Appendix 1.

Reach-Scale Time Series Data Collection

The study reach is located at East Branch Amity Creek in the city of Duluth, just upstream of the confluence (elevation 1002 feet; Lat: 46.858N, Long: 92.032W) with Amity Creek. Stream temperature, level, and flow data were obtained for East Branch Amity Creek from the MPCA gage station H02037005, located at the upstream border of the reach area (Fig. 4). Downstream of the gage, a total of nine monitoring wells were installed in the floodplain to measure hydraulic heads in the shallow aquifer adjacent to the stream (Fig. 4). Four of the wells were placed into and along the banks of a remnant channel, located to the east of East Branch Amity Creek. Surficial flow in the remnant channel is stagnant during low to moderate flows due to inactive beaver dams found downstream. Monitoring wells consisted of 2 inch outside diameter PVC pipe with 3 inch bottom screen and a HDPE well cap, fitted to allow venting to the atmosphere. Seven wells were installed to depths of 2.96 to 3.67 feet below ground surface with coarse material back-fill surrounding the screen. Two wells were installed to lesser depths, well 14+00 (2.39 feet) and well 11+10 (2.33 feet), due to restrictive soils. Area soils were a mix of sand, gravel, and clay till.

Onset HOBO data loggers recorded water level and temperature data at 15 minute intervals. A data logger was also deployed in air, near monitoring well 12+00. Wells that logged complete ice-free seasons in years 2010 to 2013 are shown in Table (1a) and wells with seasonal data gaps are identified in Table (1b). Top-of-casing and ground elevations were surveyed using a Trimble R8 GNSS (Global Navigation Satellite System). Bottom of well and periodic depth to water were measured using a steel tape with 0.01 feet accuracy.

Table 1. Groundwater level logger deployment summary

1a. Complete Seasons - dates of deployment

2010	all wells	July 1 - November 16
2011	all wells	April 9 - November 1
2012	8+00	Mar. 20 - November 7
	12+00	
	13+00	
2013	4+00	April 26 - November 5
	11+00	
	12+00	
	13+00	

1b. Data Gaps - dates of no deployment for wells with incomplete seasons

2012	4+00	March 20 - May 2	late deployment (access issues)
	10+25	August 21 - November 7	dry well
	11+00	May 30 -July 27	no deployment
	11+10	March 20 - May 2	late deployment (access issues)
	11+10	June 23 - November 7	dry well
	14+00	August 21 - November 7	dry well
	15+00	Sep 11 - November 7	dry well
2013	8+00	all season	no deployment
	10+25	all season	no deployment
	11+10	all season	no deployment
	14+00	all season	no deployment
	15+00	all season	no deployment

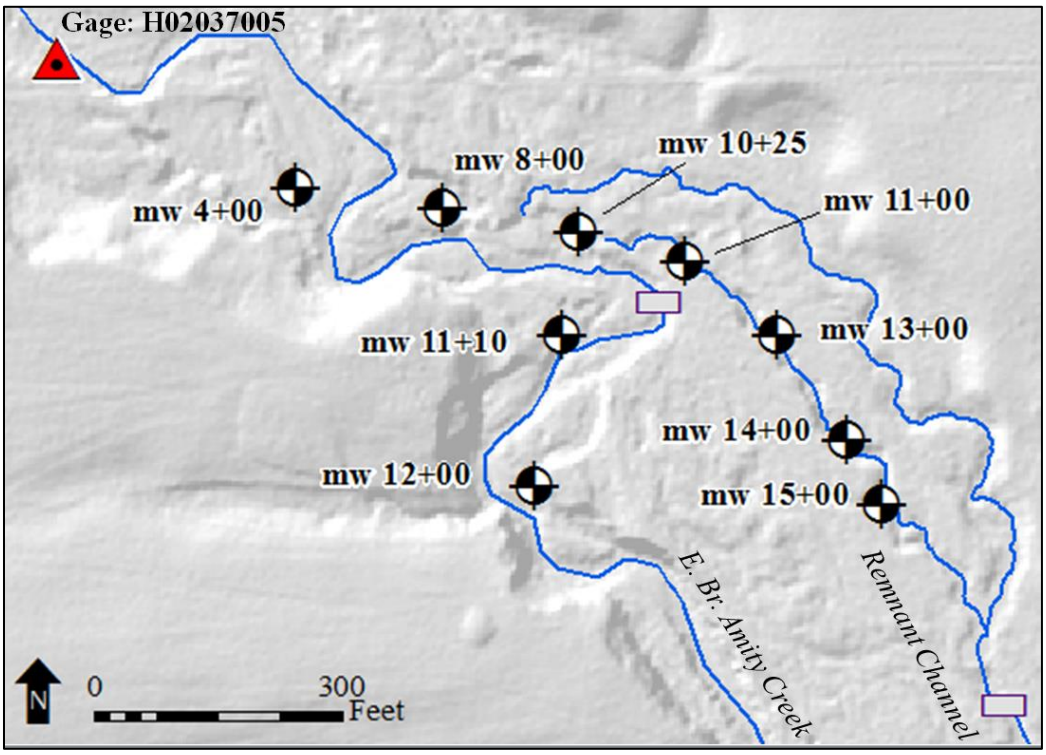

Figure 4. Map of Study Reach showing monitoring well locations, East Branch Amity Creek flow gage (triangle) and inactive beaver dams (rectangles).

Reach-Scale Isotope Sample Collection

Isotope samples of shallow groundwater were collected from monitoring wells (Fig. 3) periodically throughout the study timeframe, capturing snowmelt, rain, and baseflow conditions. Wells were pumped two times the total well volume prior to collection into a 125 to 250 mL HDPE bottle. Surface water samples from the stream and remnant channel (Fig. 3) were collected according to methods outlined previously in the Watershed-Wide Isotope Sample Collection section.

.

ANALYTICAL METHODS

Watershed-Scale Isotope Characterization

Precipitation.

Interpretation of the isotopic composition of precipitation has been done for decades to help characterize source water and define end-members to groundwater and surface water systems. The global meteoric waterline ($\delta^2H = 8.17* \delta^{18}O + 11.27$), developed by Craig (1961) and refined by Rozanski et al. (1993) defines a linear relationship between $\delta^{18}O$ and δD in meteoric waters worldwide; however this relationship can vary geographically. Because precipitation is a dominant input in this particular shallow groundwater system, it was critical that a local meteoric waterline (LMWL) was developed for this study. Meteoric water relationships with air temperature and landscape elevation were also evaluated. Deuterium- excess ($d = \delta^2H - 8*\delta^{18}O$), first proposed by Dansgaard (1964) as an offset of meteoric waters from the GMWL, was calculated for precipitation samples (Table A1-1). Globally, d averages 10‰ (Clark and Fritz, 1997), but a typical range for temperate continental climates is 0‰ – 20‰ (Gammons et al., 2006). A change in d-excess indicates secondary processes in the atmosphere with high values indicating an addition of depleted moisture to the atmosphere, typically from evaporation of open waters, and low values representing evaporation of condensed water within a dry air column.

Evaporative Loss Analysis of Baseflow.

Low flow periods typically occur during late summer and early fall when evapotranspiration in local streams plays a critical role in the water budget. Examined experimentally and theoretically (Craig and Gordon, 1965; Gonfiantini, 1965), it has been shown that surface waters that have undergone evaporation are typically enriched in $\delta^{18}O$ and δD. This is the result of lighter isotopes more easily entering the vapor phase and the heavier isotopes concentrating in the liquid phase. The enriched waters tend to stray from the LMWL, falling along a local evaporative line (LEL) that has a slope in the range of 4 to 6. As the fraction of water lost to evaporation increases, points increasingly and proportionately plot to the right, showing more enrichment.

Nine watershed-wide stream samples and one remnant channel surface water sample collected under severe drought conditions in September 2012 were used to develop a LEL for the Amity Creek watershed and analyze trends. A lakes model, outlined in Gibson et al. (2002) and Gibson and Reid (2010), designed to estimate percent water loss by evaporation for open bodies of water, was applied to the September 2012 stream isotope data. Acknowledging that the steady state conditions applied to lakes may not apply exactly to stream systems, the model was used to approximate quantitative differences between stream watershed locations in this study.

Details of equations and variables used in the model are outlined in Appendix 2. Relative humidity, air temperature, and water temperature are environmental inputs to the model. Mean values for the ice-free season, April to October 2012, when evaporative

processes on open water would be occurring, were used. Mean relative humidity (0.66) was provided from the Duluth International Airport weather station. Mean water temperature (12.96°C) was reported from the East Branch Amity Creek stream gage (H02037005) and mean air temperature (13.33°C) was recorded from the ambient air data logger deployed at the study reach.

Watershed-Scale Flow Comparison

A flow comparison of Amity Creek and East Branch Amity Creek was completed for years (2011 – 2012) with concurrent flow records. The East Branch Amity Creek sub-basin covers 48.6% of the Amity Creek watershed area. Acknowledging that flow contribution of East Branch Amity Creek to Amity Creek may vary seasonally, flow regimes were first established using flow records for Amity Creek gage (H02038001) from 2002-2012. For each flow regime, the ratio of the East Branch Amity Creek flow (gage, H02037005) to Amity Creek flow at 15 minute reporting intervals was computed. Where 15 minute data were missing from either gage, the data were excluded from the analysis. The median value of computed ratios was the final output for each flow regime.

Reach-Scale Time Series Analysis

Groundwater depth to water duration curves using mean daily records (n=206) were calculated for monitoring season 2011, the only monitoring year with a complete seasonal record for all wells. Duration curves were analyzed for similarities and differences in seasonal and annual flow patterns to aid in identification of potential

groundwater storage zones within the study reach and then grouped accordingly. Based on zone characterization of wells, land surface features were considered as geomorphic controls on groundwater storage. Using median daily values of depth to water for all wells within a grouping, a representative duration curve of each storage zone was developed. Magnitude, shape, and comparison of curves was used to identify groundwater flow regimes that were then applied to further interpret time series data including interactions with surface water and seasonal variation within the surface water – groundwater system. To compare hydrograph response to precipitation amount, rainfall totals at 15-minute intervals were estimated at the study reach using inverse distance weighting of two regional rain gage stations: MPCA-H02036003 (Lat 46.88N: Long: 91.99W), and city of Duluth-Lakeside (Lat: 46.83N, Long: 92.01W) gages. The gages are located respectively 2.75 and 1.82 miles from the study reach.

The two storage zones defined in this study include near-bank groundwater (NBGW) and depressional groundwater (DGW). The NBGW zone is representative of bank storage, defined as a location of frequent interaction between a stream and the adjacent groundwater zone (Winter et al., 1998). As defined, stream water moves into this zone during periods of rapid rise in surface water elevations and typically returns to the stream within days to weeks. If stream levels rise above bankfull elevation, excess flow into the floodplain could result in DGW storage. In depressional storage, groundwater is recharged by water captured on the land surface and infiltrated through the soil profile. Snowmelt, rain events, and above bankfull conditions are the dominant

source inputs. Depending on the system, water returns to the stream may take weeks, months, or years.

Reach-Scale Isotope Characterization

Lateral and longitudinal flow contributions to the study reach were evaluated for isolated events including snowmelt, rain stormflow, baseflow in a normal year, and baseflow during a severe drought using isotope analysis. Potential source waters evaluated included upstream inputs and lateral surficial and subsurface flow inputs. Percent contribution of runoff and baseflow were estimated using a linear mixing model. Model inputs included the isotopic composition of rain, snow, and surface water samples that fell on the LMWL in addition to the initial inflow value (δ_I) equal to the intersection of the LEL and LMWL.

RESULTS

Isotope Characterization of Precipitation

The isotopic composition of 64 samples collected in the Amity Creek watershed of Duluth, MN, are provided in Appendix 1, along with air temperature and relative humidity information for each sampled precipitation event. Maximum and mean daily values for air temperature (°C) and relative humidity (%) are reported from the weather station located at the Duluth International Airport (Lat: 46.84N, Long: 92.23W). While the majority of the isotope results for precipitation fall within a range of $\delta^{18}O$ (15‰) and δD (125‰), a cold-air event collected on November 24, 2012, expands the total range of $\delta^{18}O$ (22‰) and δD (182‰). A plot of $\delta^{18}O$ for precipitation (rain and snow) vs. mean

daily temperature, using the mean isotopic composition of snow for sample dates April 1, 2011, and March 12, 2012, shows a positive linear relationship (Fig. 5). A moderate correlation is observed ($r^2 = 0.60$) and the resulting slope (0.53‰ per ºC) is similar to values obtained in other studies (Gammons et al., 2005 & Harvey and Welker, 2000).

A local meteoric waterline (LMWL, $\delta D = 8.4 * \delta^{18}O + 15.5$, $r^2 = 0.98$) is developed using 20 precipitation samples, collected in years 2011 and 2012. Points plot on a line ($r^2 = 0.98$) with a slope and intercept slightly higher than the global meteoric waterline (Fig. 6). The Duluth LMWL falls within range of waterlines observed in published regional studies including lines developed for Moorhead, Minnesota, (slope = 7.8, intercept = 9, Magner et al., 2001) and Québec, Canada (slope = 8.8, intercept = 22, Sklash and Farvolden, 1982). Respective high (24.56‰) and low (-7.37‰) deuterium excess values are observed for April 15, 2012, and September 19, 2012, precipitation samples. These d values are outside the thresholds of a typical range (0‰ – 20‰) observed in temperate climates (Gammons et al, 2006). The d-excess range for the remaining precipitation samples is 5.95‰ to 16.60‰.

April 2011 and March 2012 samples show that the isotopic composition of snow varies across a watershed. On a plot of oxygen-18 versus elevation, a good correlation is observed in 2011 ($r^2 = 0.82$) and a fair correlation in 2012 ($r^2 = 0.56$). In both events, the isotope signature for surface water station SW22, located nearest to Lake Superior, shows the most enrichment and the composition for site SW17, East Branch Amity Creek headwater, shows the greatest depletion.

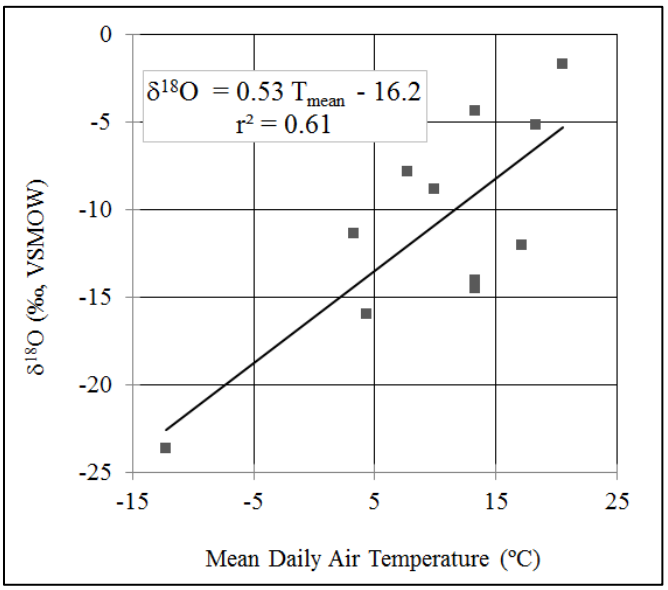

Figure 5. Relationship of $\delta^{18}O$ (‰ relative to standard VSMOW) and mean daily air temperature (°C). The mean isotopic composition of snow represents the $\delta^{18}O$ value for sample dates April 1, 2011, and March 12, 2012. A rainwater sample from April 1, 2011, is included in the analysis as a separate datum point.

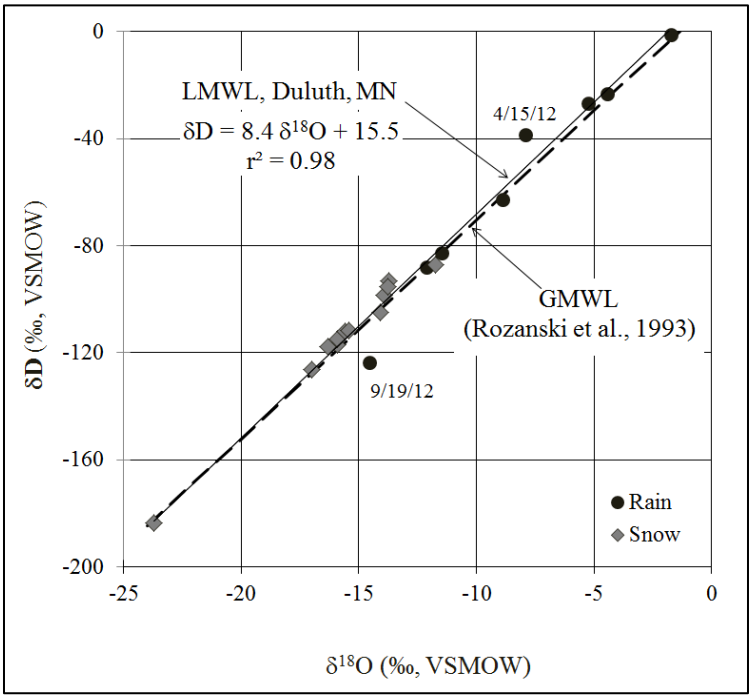

Figure 6. The local meteoric water line (LMWL) for Amity Creek watershed, Duluth, MN, displayed with the global meteoric water line (GMWL) (Rozanski et al., 1993).

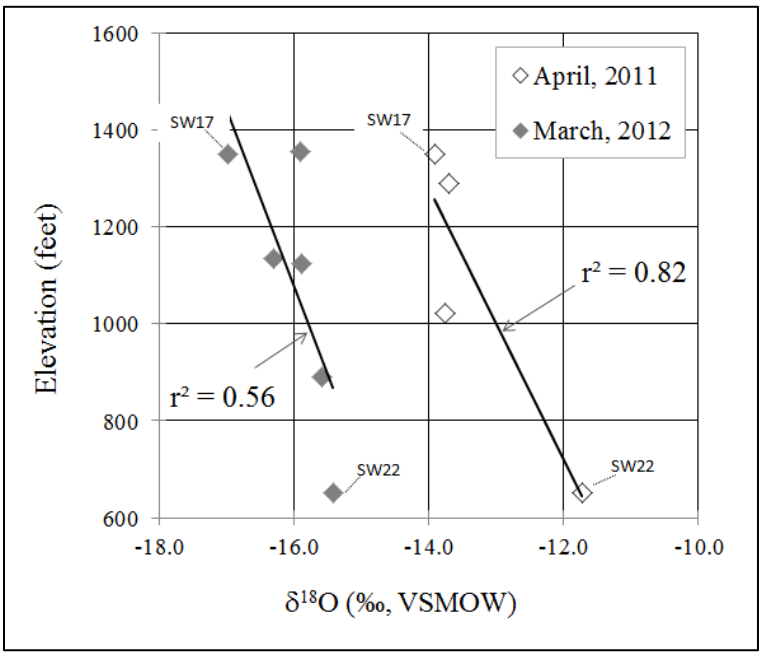

Figure 7. Relationship of $\delta^{18}O$ (‰ relative to standard VSMOW) in snow samples and elevation (feet). Enrichment of $\delta^{18}O$ in the snow pack occurs with decrease in elevation during 2011 and 2012 sample events. In both events, surface water station SW22, located nearest to Lake Superior, shows the most enrichment and site SW17, East Branch Amity Creek headwaters, shows the greatest depletion.

Watershed-Scale Isotope Characterization of Surface Waters

Surface water samples have a greater seasonal range of $\delta^{18}O$ (7‰) and δD (52‰) than the range $\delta^{18}O$ (4‰) and δD (26‰) observed in shallow groundwater. Waters with the highest enrichment, plotting on the upper-right of Figure 8, represent the May 2012 rain event. Signatures showing the most depletion plot to the lower-left and represent snowmelt sampled waters in years 2011 and 2012. In general, baseflow samples cluster centrally in the graph among groundwater samples.

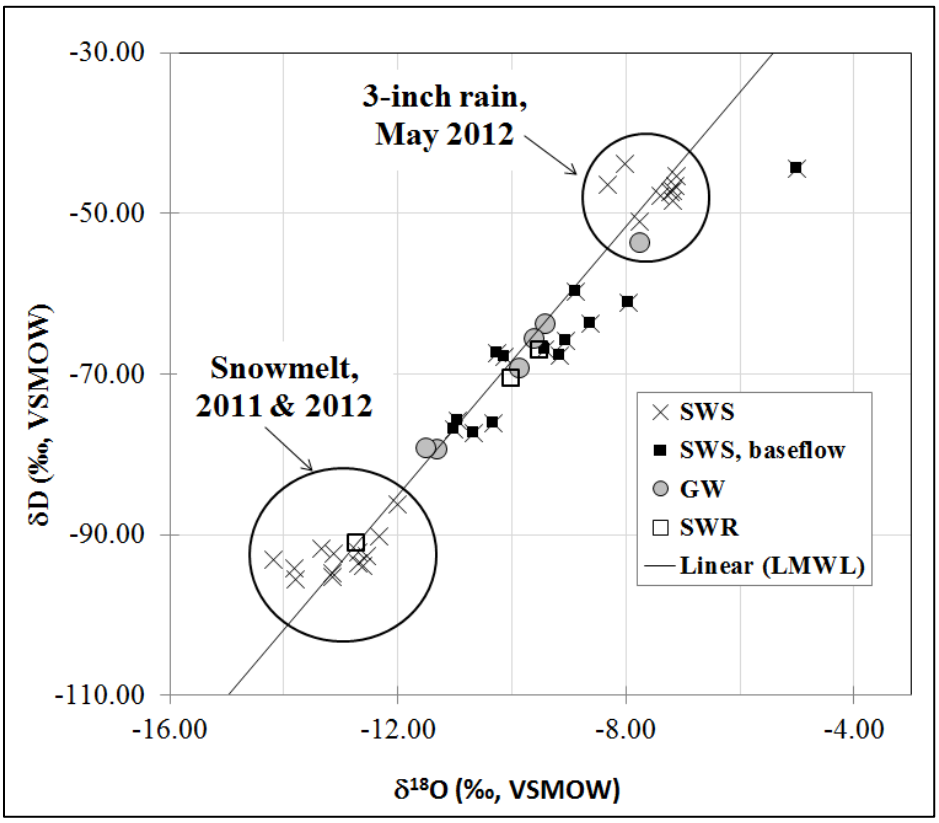

Figure 8. Isotopic Signatures of surface water (SWS) and groundwater (GW) collected during the study timeframe (2010-2013). Isotope signals influenced by large surface water events are grouped by storm event. Generally, groundwater, remnant channel water (SWR), and stream baseflow surface water (SWS, baseflow) samples cluster centrally in the graph with a portion of the points located along the LMWL and others deviating below.

Baseflow Characterization through Evaporative Loss Analysis.

Nine watershed-wide stream samples and one remnant channel surface water sample (SWR) collected under severe drought conditions in September 2012 are displayed in Figure 9. Seven of the surface water samples stray from the LMWL, forming a LEL ($\delta D = 5.21\ \delta^{18}O - 18.72$). The remnant channel surface water datum is included in LEL development as it marginally falls outside the bounds of error lines (2σ = 2 x the

maximum reported Std of $\delta_{precipitation}$) of the LMWL. Fraction of water loss is proportionate to the placement along the LEL with the most losses observed in stream site SW10. No deviation from the LMWL is observed from sites SW11, SW12, and SW13. These non-evaporative waters show more enrichment than the predicted inflow (δ_I) of well-mixed groundwater which theoretically occurs at the intersection of the LMWL and LEL ($\delta^{18}O$ = -10.83). Estimated percent water loss due to evaporation, based on the Gibson et al. (2002) and Gibson and Reid (2010) model are provided in Figure 10 and Table A2-1. Estimated evaporative losses range from 0 - 48% with more complexity and overall loss observed in Amity Creek when compared to East Branch Amity Creek.

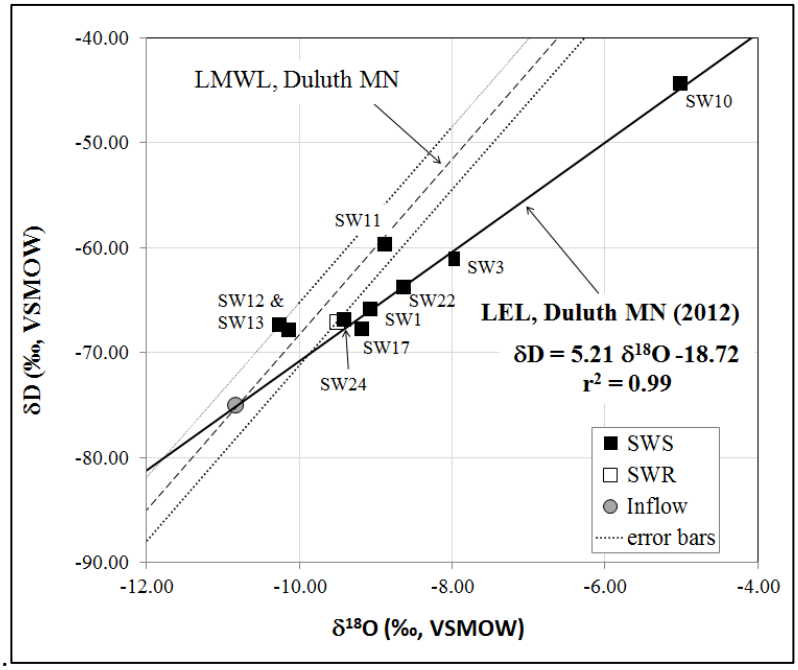

Figure 9. The local evaporative line (LEL) for Amity Creek watershed, Duluth, MN, developed with September 2012 baseflow data and displayed with the local meteoric water line (LMWL). Error bars (3‰) represent 2σ.

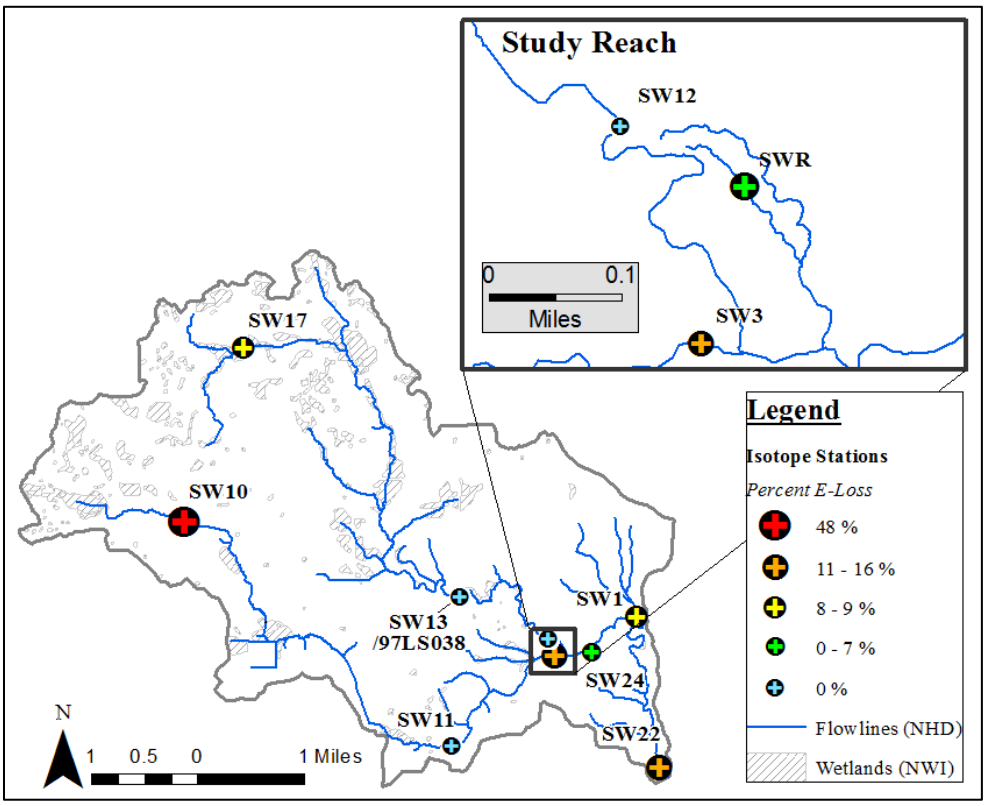

Figure 10. Map of isotope sample locations and respective estimates of percent water loss to evaporation of surface water in September, 2012. Estimates were derived from an open water body model outlined in Gibson et al. (2002) and Gibson and Reid (2010) to show quantitative differences between stream watershed locations. See Appendix 2. Flowlines are from the National Hydrography Dataset (NHD) and wetlands (from the National Wetlands Inventory (NWI). Insert map is the study reach.

Watershed-Scale Flow Comparison

Flow regimes for the Amity Creek stream gage are shown below in Figure 11. Breaks were defined by the top 10% (very high), bottom 10% (very low), and middle 20% (mid-range) flow exceedance. High flows and low flows describe the 30% range in exceedance respectively above and below the mid-range thresholds. Percent flow contribution (Table 2) of East Branch Amity Creek to Amity Creek varies with flow regime. The highest contributions (62-68%) are computed during low and mid-range

flows. Lower contributions (35-43%) are observed during very low, high, and very high flows. MPCA flow measurement records from October 8, 2010, confirm 63% contribution from East Branch Amity (1.84 ft^3/s) to Amity Creek (2.92 ft^3/s) for mid-range flows.

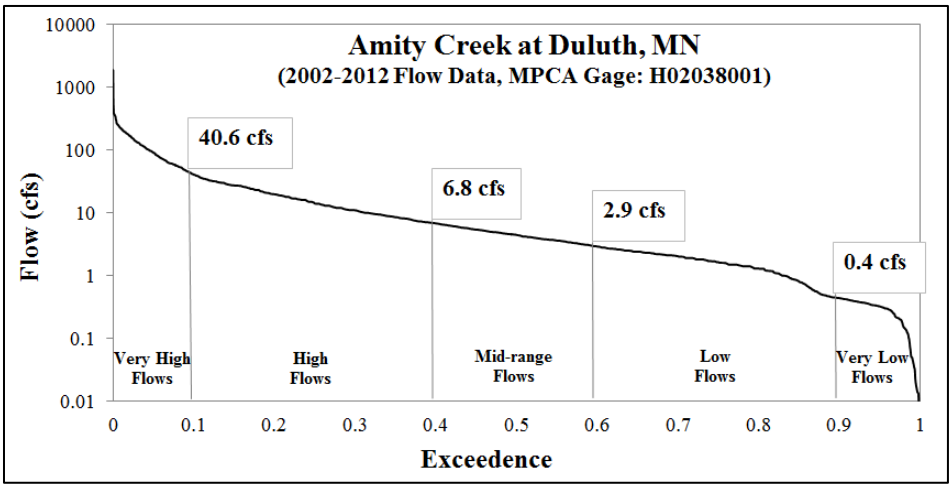

Figure 11. Flow duration curve for Amity Creek gage H02038001 with identified flow regimes for the 2002-2012 record.

Table 2. Flow contribution of East Branch Amity Creek (MPCA gage: H02037005) to Amity Creek (MPCA gage: H02038001)

% Total Flow: East Branch Amity Creek to Amity Creek, 2011-2012					
All Data	Very High	High	Mid-Range	Low	Very Low
46.1	42.6	35.9	62.2	67.8	36.4

Reach-Scale Groundwater - Surface Water Time Series Analysis

Groundwater Storage Zones.

Groundwater storage zone boundaries within the valley walls of the study reach are identified through analysis of depth to water duration curves for all monitoring wells. Two distinct patterns (Figs. 12 a & b) are observed in duration curves: near-bank groundwater (NBGW) and depressional groundwater (DGW). Five monitoring wells (4+00, 8+00, 10+25, 11+10, and 12+00) are characterized as NBGW and the remaining four wells (11+00, 13+00, 14+00, 15+00) as DGW (Figs. 12 & 13). Duration curves for wells exhibiting NBGW storage are concave upward and infer flashy hydrology. DGW plots generally are much flatter, and show a distinct inflection at approximately 54% exceedance. Through analysis, duration curves for wells 4+00 and 13+00 are found to have similar placement, range, and shape to median value plots for NBGW and DGW respectively and are considered representative of the respective zones in further time series analysis.

Based on zone categorization of wells (Fig. 13), storage zone boundaries and controls are inferred. The lateral distance between NBGW wells and the stream range from 35 to 64 feet and are located within the active floodplain. The floodplain boundary (Fig. 13), depicted from LIDAR imagery using ArcGIS and field observations, is less clear in the vicinity of monitoring well 10+25 where the undulating topography appears to be an overflow route for stream water to enter the remnant channel during extremely

high flows. DGW wells are located distances 55 to 280 feet from the stream, outside of the boundary of the active floodplain, and along the perimeter of the remnant channel.

Comparison of groundwater levels to stream levels (Fig. 14) demonstrates similarities between stream and NBGW hydrographs particularly during stormflow response. While the DGW hydrograph shows equal time to peak response as NBGW and stream traces, the peak magnitude and particularly stormflow release time shows noticeable differences. This is observed during the June 21, 2011, and August 2, 2011, rain events. During the August event, DGW levels increase by 1.2 feet and stormflow release time is approximately 30 days. Water level response in the stream (3.17 feet) and NBGW (2.76 feet) are more than 2 times greater. The majority of stormflow release for the stream and NBGW occurs within 3 days and 4 days respectively.

Hydraulic head above land surface is an indicator of artesian conditions in wells. Well data indicate that artesian conditions were recorded at all wells during the 2010 to 2012 period of record (Table 3) and each well had at least one occurrence outside of the 2012 flood. Generally, this condition was recorded more often and for longer durations in the near-bank groundwater zone. In DGW wells 11+00, 13+00, and 15+00, located above the high bank of the remnant channel, artesian conditions occurred only once other than the 2012 flood; an April 2012 spring rain event on saturated soils. DGW 14+00, located within the banks of the remnant channel, experienced artesian conditions more frequently than other DGW wells.

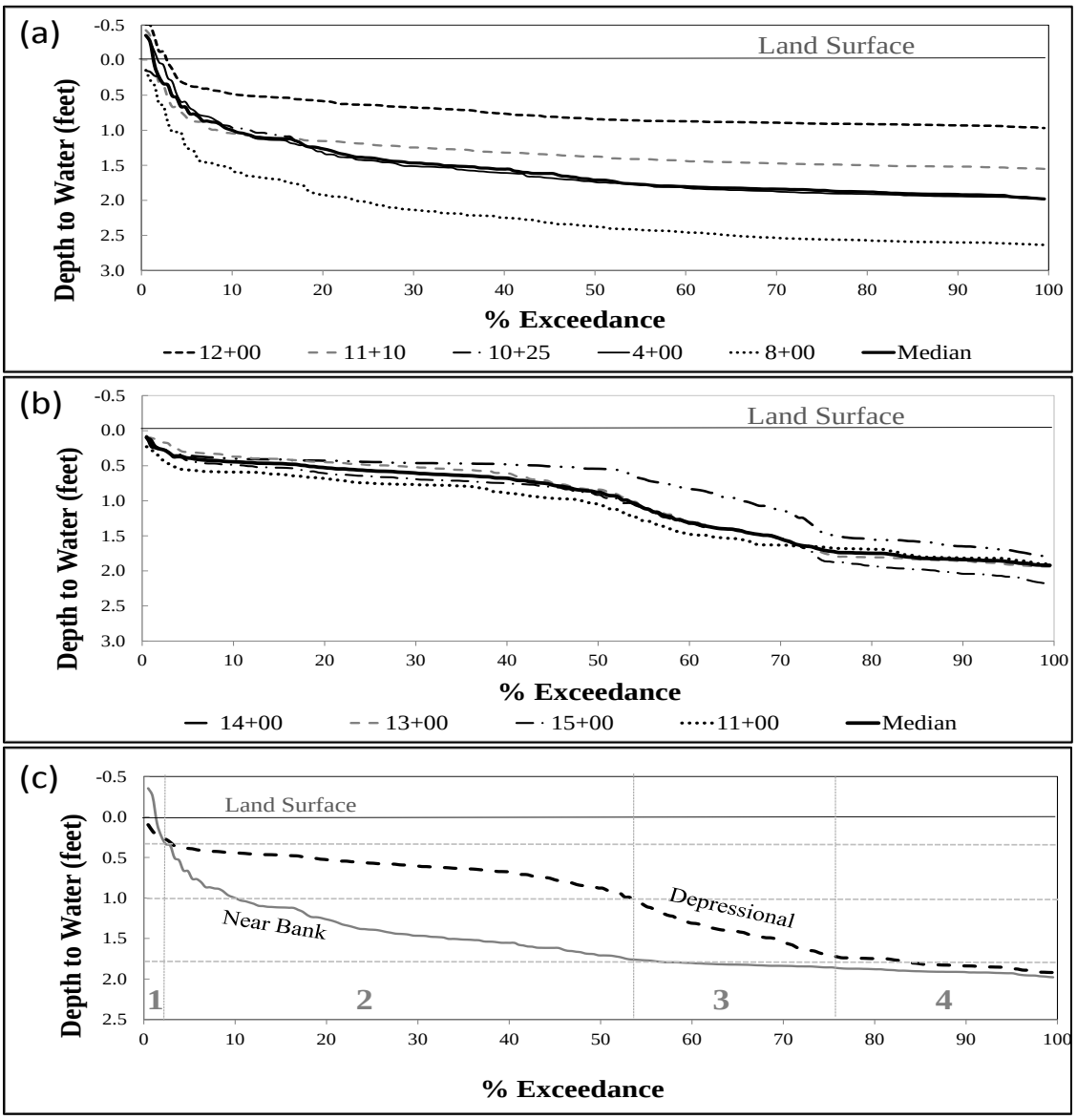

Figure 12. Groundwater depth to water duration curves for monitoring year 2011. Two distinct patterns represent hydrologic response of (a) near bank and (b) depressional groundwater storage zones. Duration curves for the median values of well comprising of each zone are displayed individually in (a) and (b); and are overlaid in (c) for comparison. Four groundwater flow regimes are identified in (c).

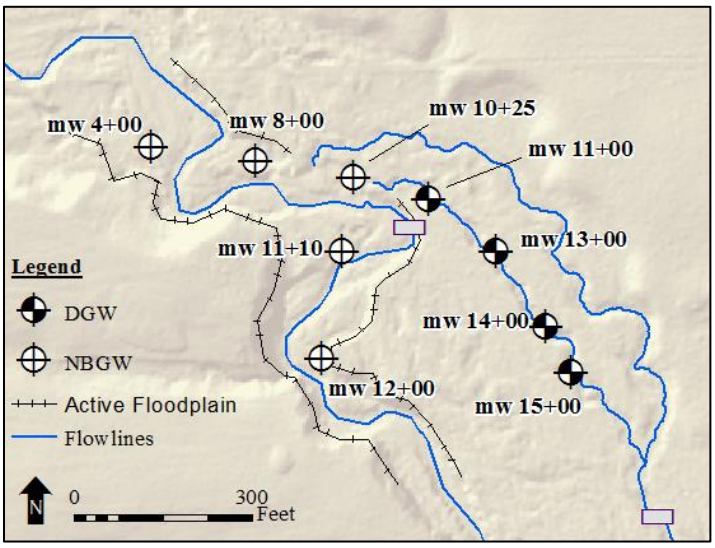

Figure 13. Map of monitoring wells located in zones of near bank groundwater (NBGW) and depressional groundwater (DGW).

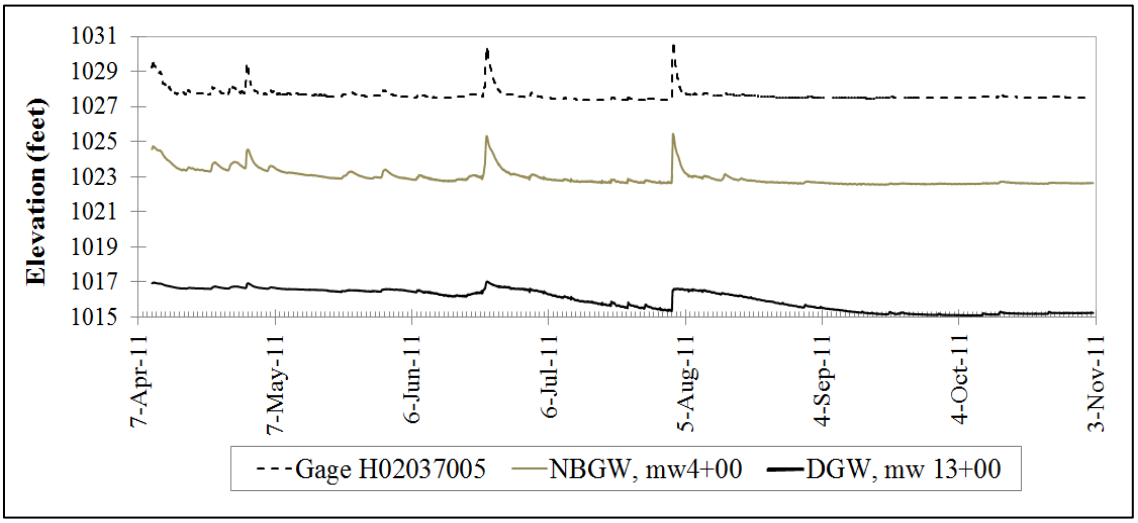

Figure 14. Comparison of groundwater and stream elevation plots (2011) showing similarities in peak magnitude and runoff response between stream and the NBGW hydrographs. DGW hydrology is less flashy with lower peak magnitudes and longer rainfall release time.

Table 3. Artesian conditions in monitoring wells: Years 2010-2012

Artesian Conditions, Years 2010-2012				
	Monitoring Well	Occurrences	Duration (Days)	% Time of Total Record
NBGW	12+00	11	14.25	2.27
	4+00	8	8.58	1.60
	11+10	7	5.25	1.27
	8+00	4	5.11	0.81
	10+25	6	3.93	0.72
DGW	14+00	6	3.41	0.65
	13+00	2	1.66	0.31
	15+00	2	1.40	0.27
	11+00	2	1.29	0.21

Groundwater Flow Regimes.

Four groundwater flow regimes are identified when median value duration curves representing near bank and depressional water levels are compared (Fig. 12c). Regimes are then projected onto time series plots (Figs. 15 b & c) of wells representing the two zones. Flow regime 1 represents extremely wet conditions during which hydraulic head with respect to land surface are greater in NBGW than DGW. While a rapid rise of the hydrograph in response to an event occurs in both zones, it is significantly more prominent in the near bank as time-to-peak occurs within hours of the initial water level rise. In 2011, this occurs less than 2% of the recorded seasonal record, lasting up to two days per occurrence, primarily during peak snowmelt and large rain events. In flow regime 2, hydraulic head is noticeably greater in the depressional zone than the near bank zone. The DGW duration curve is relatively flat while the steeper NBGW slope decreases with increase in percent exceedance. Groundwater is in this flow regime following the 2011 snowmelt, mid-April to June, during an average (40-60th Percentile) snowpack year and then again on the recession limbs of June and August rain events between 2 days and

approximately 2 weeks following the initial rain response (Fig. 15b). In 2011, flow regime 2 accounts for 52% time of the recorded seasonal record. Groundwater levels during the latter half of the June and August rain recession limbs are in flow regime 3. The slope of the DGW duration curve steepens negatively and the NBGW slope flattens as the two curves begin to trend closer together. This occurs 22% of the time in 2011. Curves plotted for both zones flatten in flow regime 4 with depth to water (DTW) in the depressional zone slightly higher. This occurs 24% of the 2011 record, during stream baseflow conditions in mid-September to mid-October.

Annual Variability.

Time series data for years 2010 and 2012 are displayed respectively in Figures 15 (a) and (c). Flow regimes developed using the 2011 data are not applied to the 2010 due to the appearance of different exchange relationships between DGW and NBGW in the 2010 data. For example, when NBGW levels approach baseflow in the latter weeks of months August and September, DGW levels remain relatively stable at a higher level (DTW < 1.25 feet) than expected (1.75 feet) for flow regime 4. Rain event response in the DGW hydrograph appears to be more buffered with less defined peaks in 2010 than following years. Another deviation from the defined 2011 groundwater dynamic occurs post-flood 2012. Levels in the DGW drop below previously recorded minimums (DTW = 1.95 feet), reaching DTW values equal to 3.38 feet, within 3.5 weeks following the peak flood (June 19, 2012). Pre-flood 2012 records appear to follow the defined 2011 flow regime dynamics.

Flood Effects.

Further examination (Table 4 and Fig. 16) of post-flood groundwater levels shows a decrease in the water table from pre-flood records (2010-2011) in a select number of wells, beginning one month after the flood and continuing through the ice-free year (2012). Wells located along the remnant channel became perched or recorded 0.94 to 1.75 feet deficits in late 2012 compared to pre-flood minimum recorded levels. Similarly, wells located downstream of a slope break, field identified near the inactive in-stream beaver dam (Fig. 4), were perched or recorded deficits of 0.84 feet during post-flood 2012. Near bank wells, located upstream of the slope break, logged negligible change (Table 4) in minimum levels between pre-flood and post-flood periods. Similar relationships are observed in 2013 deployed wells (Table 4).

Field observations on June 27, 2012, noted changes in stream channel and remnant channel geometry. Significant observed in-stream geomorphic change occurred at an existing slope break at the old beaver dam. An increase in gradient at the knick-point is noted, specifically aggradation at the upstream boundary of the break along with incision at the downstream boundary. Organics in the remnant channel are noted as being removed during the flood, and clay till banks and sand and gravel alluvium bed exposed. A post-flood head-cut in the remnant channel was visible with channel definition occurring further up-gradient, at monitoring well 10+25, than pre-flood positioning, near well 11+00. Gravel point bars were newly deposited near well 15+00. Evidence of overland flow throughout the entire valley included flattened vegetation and stormflow debris caught in trees at elevations four feet above ground level.

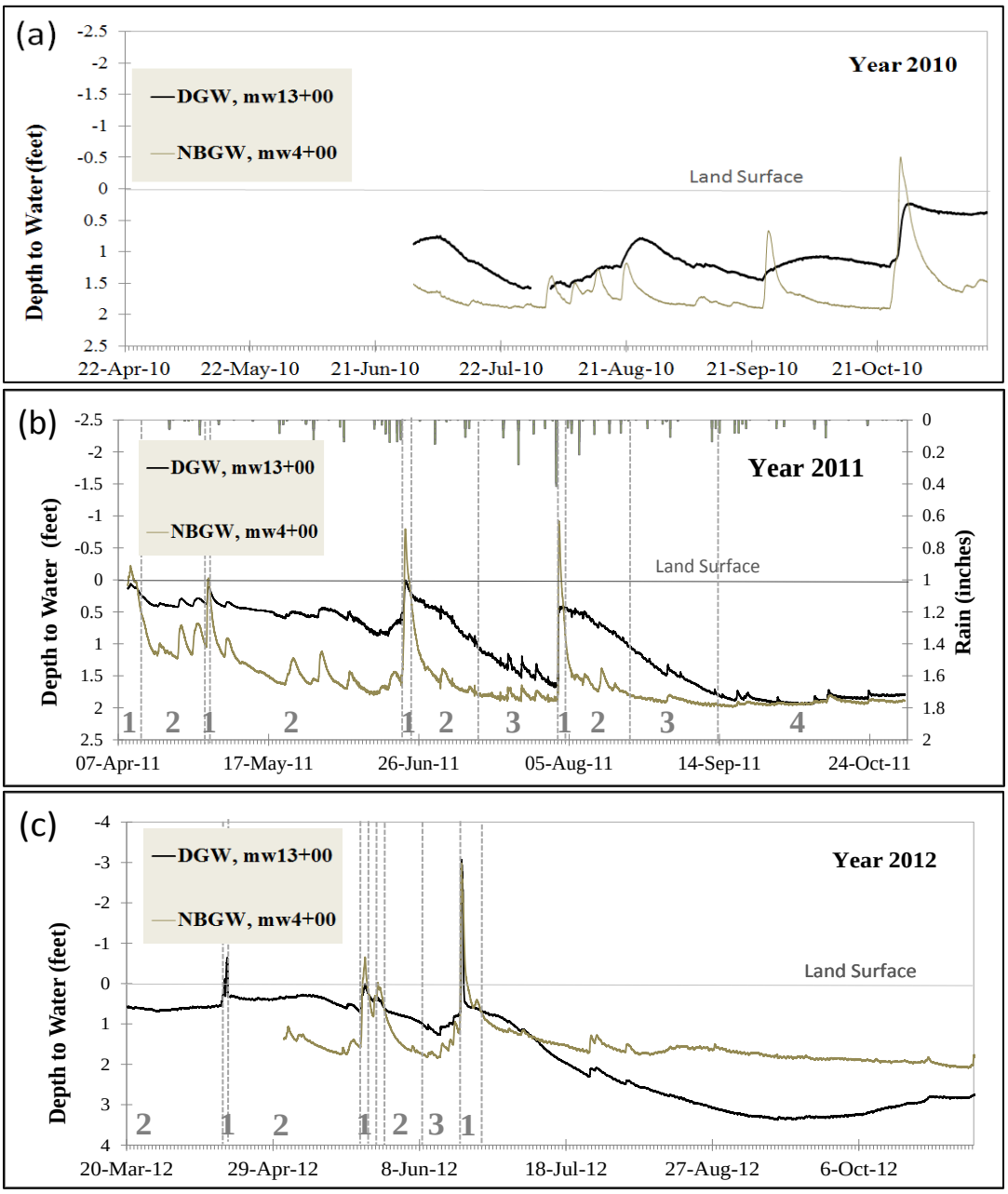

Figure 15. Near-bank (NBGW) and depressional (DGW) groundwater time series data is presented for years 2010 (a), 2011 (b), and 2012 (c). Four flow regimes developed using 2011 duration curves (Fig. 12) are applied to 2011 and pre-flood 2012 time series plots. Flow regimes do not appear to accurately represent the 2010 and post-flood 2012 exchange relationships. The vertical scale in (c) is adjusted to include maximum and minimum values and horizontal scale varies with each plot.

Table 4. Differences in Groundwater Levels between Pre- and Post-Flood Years.

	Change in minimum water levels (feet) from pre-flood years, 2010 -2011								
	4+00	**8+00**	**10+25**	**11+10**	**12+00**	**11+00**	**13+00**	**14+00**	**15+00**
Y2012	-0.11	-0.26	> -0.94*	> -0.77*	-0.84	-1.75	-1.43	> -0.57*	> -1.12*
Y2013	0.17				-0.6	-1.01	-1.02		
ZONE	NBGW	NBGW	NBGW	NBGW	NBGW	DGW	DGW	DGW	DGW
POSITION	US	US	US/R	DS	DS	R	R	R	R

US = upstream of slope break DS = downstream of slope break R = Remnant Channel

* indicates the well went dry

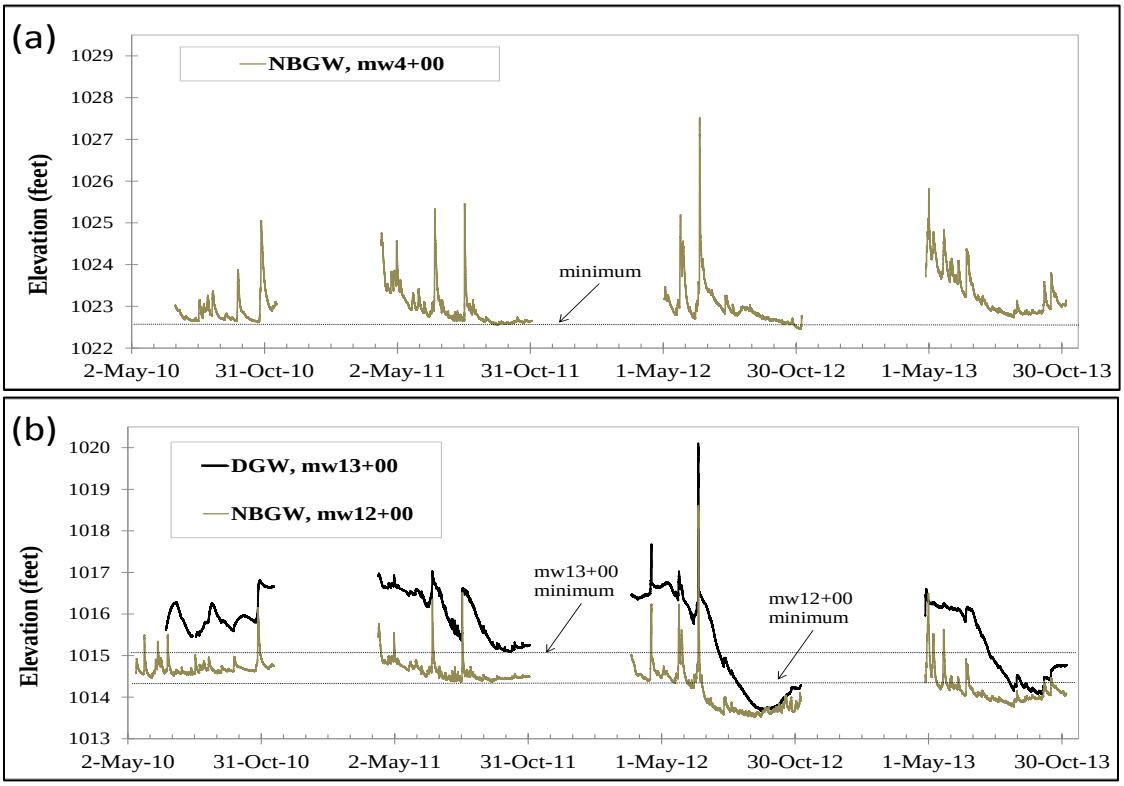

Figure 16. Pre- and post-flood groundwater levels for given wells located (a) upstream and (b) downstream of a major slope break in the stream profile. Horizontal lines identify minimum water levels recorded pre-flood. Water levels significantly drop below pre-flood minimums in (b) late summer to fall months of post-flood years.

Reach-Scale Isotope Characterization of Surface Water and Groundwater

Lateral and Longitudinal Inputs.

Lateral and longitudinal flow contributions to the study reach were evaluated for isolated events over varying conditions using isotope analysis. Isotope analysis of stream water during varying climatic conditions shows a correspondence (Figs. 17 & 18b) between the study reach (SW12) and upstream surface water station SW13. A similar relationship is observed between the study reach and stream station SW17 (Fig 17), the headwater wetland to East Branch Amity, with the exception of the September 2012 drought. During the extremely dry conditions, the SW17 signature deviates from SW12 and SW13 through enrichment along the LEL.

Lateral inputs are more complex and show variations in relationships of end members and stream water throughout seasons (Fig. 17). Beginning in 2012, the DGW signal remains relatively unchanged from its positioning near the intersection of the LMWL and the LEL (theoretical inflow value, δ_I) during snowmelt ($\delta^{18}O$ = -11.5‰) and through the May 2012 rain event ($\delta^{18}O$ = -11.3‰). During this period, it is isolated from surface water and other groundwater signals. In contrast, stream water (SWS) shifts from a depleted signal ($\delta^{18}O \approx$ -13‰) to an enriched signal ($\delta^{18}O \approx$ -8‰) during the respective snowmelt and rain events. Remnant channel surface water (SWR) shows depletion similar to surface water during snowmelt 2012, but remains buffered near δ_I during rain event conditions of 2012. NBGW signal is approximately equal to surface water during the May rain event, whereas some level of isolation from stream water is observed during

baseflow 2010 ($\Delta\delta^{18}O = 0.8‰$) and drought conditions of 2012 ($\Delta\delta^{18}O = 0.5‰$). Near-bank groundwater was not collected during snowmelt.

The tightest range (0.8‰) in $\delta^{18}O$ values observed between SW12 and all contributing source waters in 2012 occurs during September drought (baseflow) conditions, just three months after a major flood event. Baseflow 2010 also shows a relatively tight range (1.1‰) in $\delta^{18}O$ values, but the full range may not be accurately represented as the remnant channel, SW13, and DGW were not sampled. September 2012 is the only shift from the theoretical inflow value ($\delta_{I;\ intersection}$ of LMWL and LEL) observed in DGW and baseflow stream water samples. Other signals approximately equaling δ_I include SW17 during baseflow 2010 and SW13 during baseflow of 2014.

Flood Effects.

Plots of oxygen isotopes ($\delta^{18}O$) versus time show changes in the composition of source water and stream water, and their relationships as result of the flood (Fig. 18). Stream water follows a similar trend as NBGW and upstream (SW13) inputs pre- and post-flood (Fig. 18b). Baseflow data show stream water near the inflow value in November 2010 and slightly more enriched post-flood 2012. Pre-flood DGW signals show slight depletion from δ_I and are buffered from stream and remnant channel water. Post-flood, the DGW shows more enrichment at a value equal to signals observed in NBGW and remnant channel surface water (Fig. 18a).

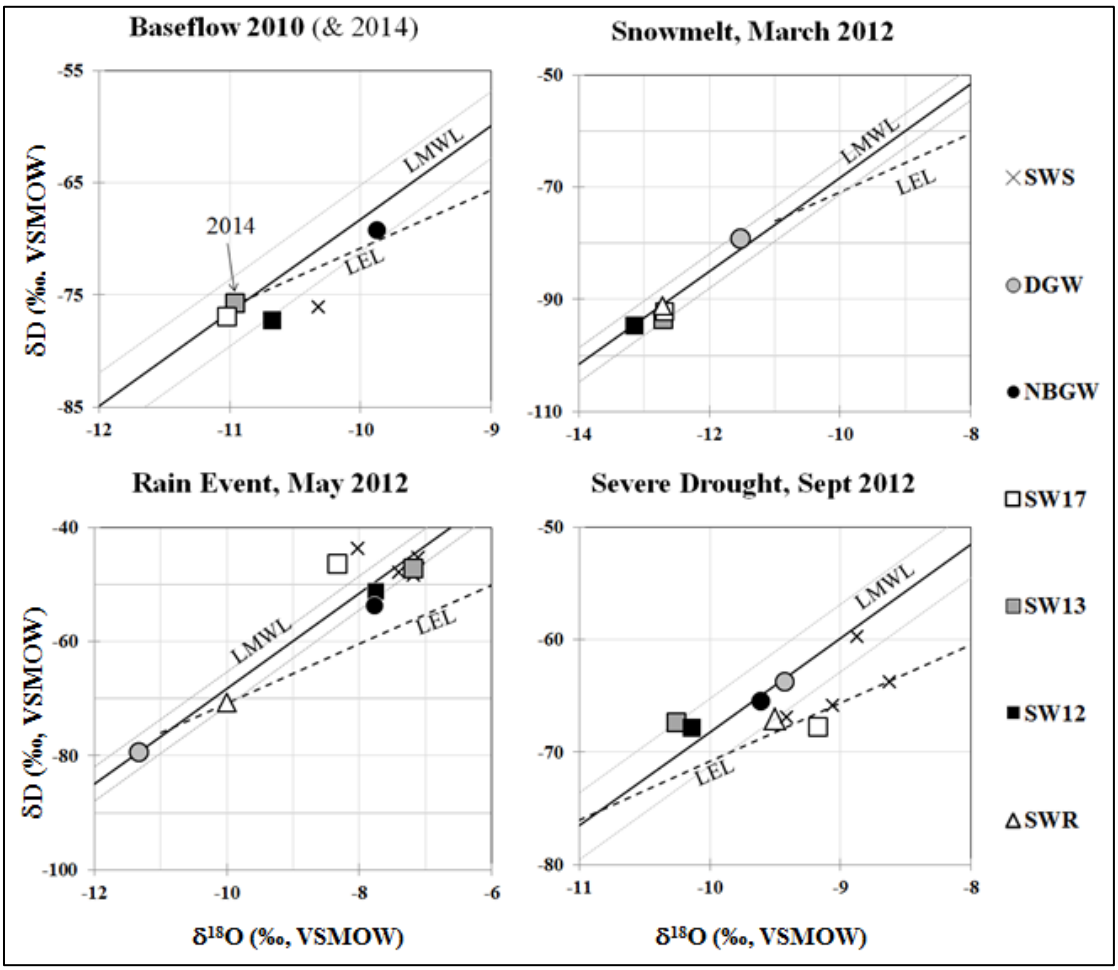

Figure 17. Reach-scale isotope signature plots of surface water and groundwater including East Branch Amity Creek at the study reach (SW12) and source waters. Source waters include longitudinal inputs from upstream surface water (SW13 and SW17) and lateral inputs of surficial (remnant channel, SWR) and subsurface (depressional groundwater, DGW; and near bank groundwater, NBGW) flow. Additional surface water samples (SWS) from Amity Creek and East Branch Amity Creek that fall within the axis range of the plots are included. A greater range in scale is plotted for March and May, 2012 and axis shifts occur between plots.

Runoff Contributions to Event Flow.

A linear mixing model using the isotopic composition of stream surface water (SW12 and SW13), baseflow (δ_I = -10.83‰), and precipitation yields estimates (Fig. 19) of percent contribution of precipitation and baseflow for a single point in time during the

two events, snowmelt and May rain, sampled in 2012. Post rain event analysis, monitored one week following the 3-inch rain event, yields approximately equal contributions from rain water runoff (46.5 %) and residual baseflow (53.5%). Snowmelt yields slightly greater snowpack contributions (58.7 %) than baseflow contributions (41.3%) three days after peak snowmelt, measured near the base of the falling limb on the hydrograph. Based on time series analysis (Fig 15c), the hydrograph is in groundwater flow regime 2 during both sample collection dates. One day prior to the May sample date, the system was in groundwater flow regime 1.

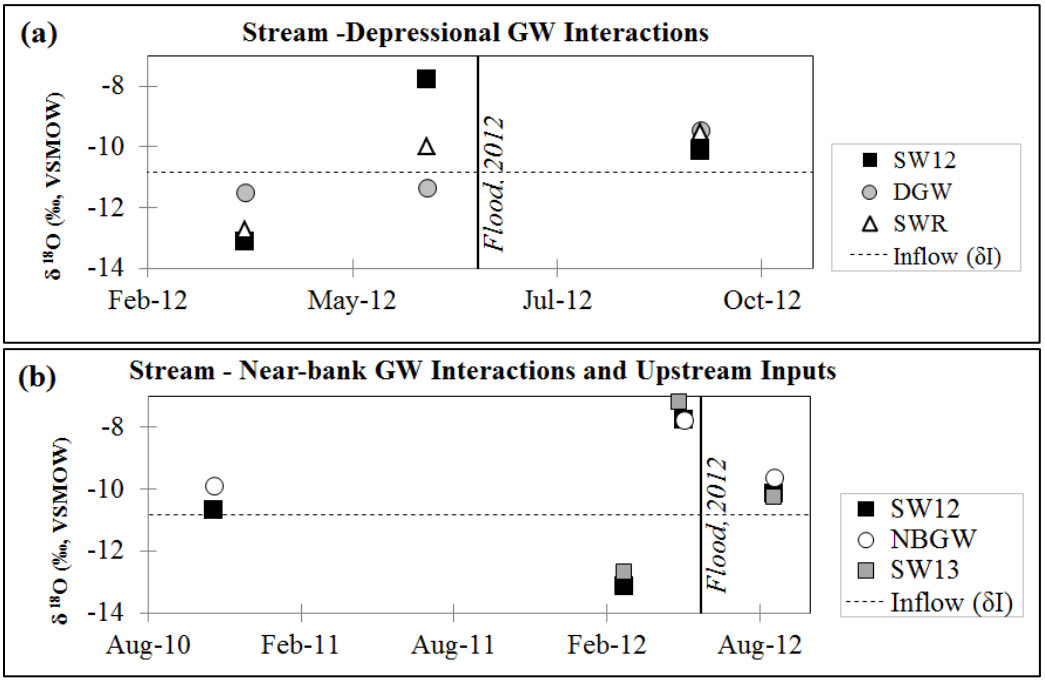

Figure 18. Isotope Signature Plots: Pre- and Post-Flood. Study reach stream water (SW12) compared to (a) depressional groundwater (DGW), remnant channel water (SWR), and theoretical inflow; and (b) near-bank groundwater (NBGW), upstream inputs (SW13), and inflow. Horizontal scale varies between plots.

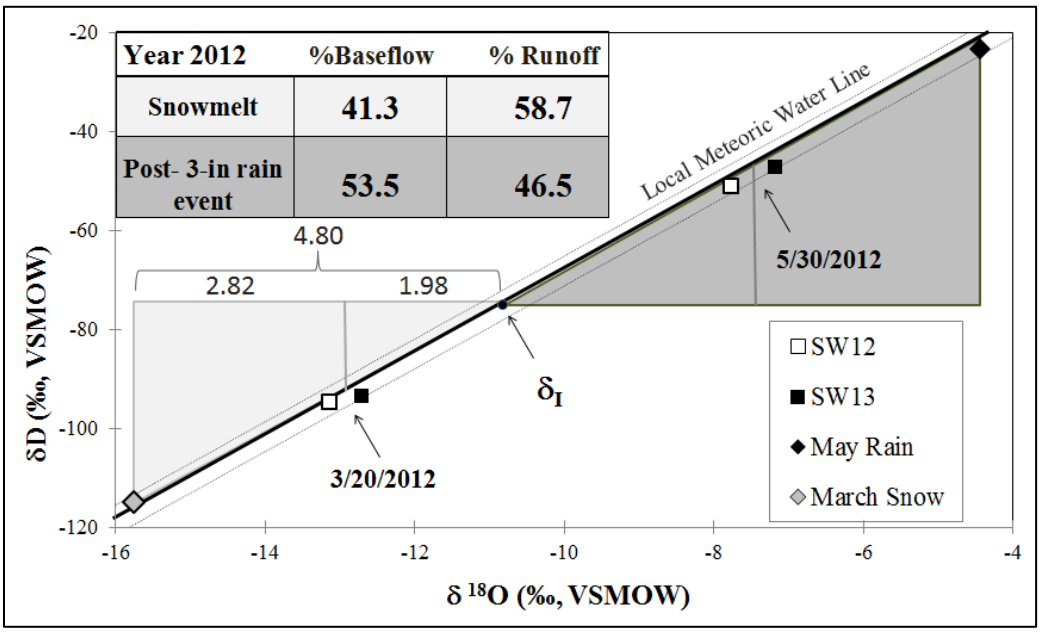

Figure 19. Isotopic linear mixing model estimates of source water (baseflow and precipitation) contributions to stream surface water during runoff events. The inflow value ($\delta^{18}O$ = -10.83) represents baseflow inputs. Snowpack and rain water data points associated with respective March and May 2012 events represents runoff inputs.

DISCUSSION

The results of this study characterize groundwater - stream water exchange at watershed and reach-scales. Seasonal variations of source-water mixing in stream water and identification of dominant groundwater discharge to stream flow is interpreted at a watershed-scale through analysis of the isotopic signatures of precipitation and stream surface water. A detailed study of exchange relationships at a reach-scale is accomplished through additional stable isotope analysis, including evaluation of groundwater and off-channel surface waters in the stream riparian; and examination of continuous water levels within the stream channel and adjacent shallow aquifer. Seasonal and flood-induced changes in groundwater – surface water dynamics are assessed at the reach-scale. Details revealed regarding regional climatic processes, including evaporation and condensation

of secondary atmospheric moisture help explain the local water budget and intricacies of source water mixing.

Isotope Characterization of Precipitation

A seven year study of the isotopic composition of precipitation in Canada shows that the slope of the meteoric water line and the intercept vary regionally, seasonally, and annually with climate region (Fritz et al, 1987). Clark and Fritz (1997) conclude that this imparts the need for LMWL development in groundwater studies. The Duluth LMWL, developed in this study, is the only known meteoric line for the North Shore of Lake Superior. It is defined by 20 precipitation samples with the majority of samples collected in 2012, the same year as the bulk collection of surface water and groundwater samples. A fair correlation between temperature and $\delta^{18}O$ for all precipitation samples and a fair to good correlation with elevation for snow samples in respective years 2012 and 2011 is observed. This implies multi-dimensional environmental controls with annual variability on the isotopic composition of condensation in Duluth, MN.

Deuterium excess in precipitation signatures for collection dates April 15, 2012, (d = 24.56‰) and September 19, 2012, (d = -7.37‰) are outside the thresholds of a typical range (0‰ – 20‰) observed in temperate climates (Gammons et al, 2006) and may be the result of secondary atmospheric processes. A high d value, as observed in the April event, indicates the addition of depleted moisture to the atmosphere from the evaporation of open waters. Thunderstorms producing greater than 2 inches of total rainfall and winds (ENE) off the lake at speeds 19-36 mph and gusts 51 mph are

associated with the event. Given the storm conditions and proximity to the lake, the source of secondary vapor flux is likely Lake Superior. Although d-excess values greater than 20‰ aren't typical, they have been observed in other Great Lakes region studies including Kalamazoo, MI (Machavaram & Krishnamurthy, 1995) and Coshocton, OH (Froehlich et al., 2002) and may be a tracer of "lake effect" precipitation. The low d value observed in September 2012 is typical of condensation that has undergone evaporative processes in the air column as it falls to land. This is possible during the cold-air, low humidity September rain event that occurred during a severe drought following months of negligible rain.

Watershed-Scale Isotope Characterization of the Surface Waters

Seasonal and spatial variability of source water mixing in stream surface waters is reflected in movement of isotopic data points along the LMWL between snow and rain runoff events and displacement along both the LMWL and LEL during baseflow conditions. The wide range in isotopic signatures in Amity Creek and East Branch Amity Creek stream waters is indicative of watersheds with limited storage and fast hydraulic residence, reflective of the flashy nature of western Lake Superior streams. Stream water with the highest enrichment is observed in data representing a 3-inch rain runoff event in May 2012. An isotopic linear mixing model (Fig.19) estimates percent runoff (46.5%) and percent baseflow (53.5%) in stream water one week after the hydrograph peak of this event. More depleted stream waters are found during the 2012 snowmelt response and percent runoff (58.7%) and percent baseflow (41.3%) are estimated for day 3 following

the peak hydrograph using the same linear model. The two events were collected near the falling limbs of the peak hydrographs which is indicative of the end of overland flow (Fetter, 2001). This suggests that baseflow is contributing a large percent of streamflow on the falling limbs of storm events, demonstrating further how quickly water moves through the system. A considerably higher percent runoff contribution is likely for the peak time of these events and could be further defined through future intensive storm hydrograph sampling.

Baseflow Characterization through Evaporative Loss Analysis.

Spatial variability of isotopic signatures in stream water is observed in all watershed-wide synoptic sampling events, however the greatest spread of points during a single event is observed during drought baseflow conditions of 2012. The isotopic composition of baseflow in stream waters, collected across the Amity Creek drainage in September 2012, fall along one of two lines: the LMWL or the LEL with a lesser slope (5%). The placement of baseflow stream waters along the LMWL is suggestive of meteoric waters that have limited exposure to the atmosphere, such as condensation that quickly infiltrates through the soil medium and into subsurface storage zones. Points falling along the LEL are representative of open water systems that have undergone non-equilibrium evaporation through exposure to a dry air environment (Clark and Fritz, 1997). Probable causal conditions for stream waters showing no sign of evaporative loss include higher stream residence times and associated groundwater upwelling near the collection site. Waters showing signs of evaporative flux to the atmosphere likely lack

dominant groundwater inputs, resulting in diminished flow, longer residence times, and areas of stagnated waters during dry periods.

In this study, presumed areas of strong groundwater upwelling, defined by no evaporative losses to the atmosphere, include Amity Creek site SW11 and East Branch Amity Creek sites SW12 and SW13. Sites SW11 and SW13 are located at stream elevation 1130 feet AMSL and the surrounding landscape features for both sites include upland drainages with high topographic relief. Deltaic sediment features with maximum elevations of 1175 to 1185 feet AMSL are visible using digital elevation maps in the area immediately adjacent to the stream at site SW13 (Biological Station 97LS038). A similar signal ($\Delta\delta^{18}O = 0.11‰$, $\Delta\delta D = 0.49‰$) to SW13 is observed at the downstream study reach (site SW12) during the September sampling indicating a common source water. Station SW12 is located at 1020 feet AMSL and approximately 0.25 miles downstream of the glacial Lake Duluth shoreline. A difference ($\Delta\delta^{18}O = 1.38‰$, $\Delta\delta D = 7.65$) from the isotopic composition of SW13 at site SW11 suggests upwelling from a different groundwater storage zone. Based on the location of these three sites, we believe that groundwater inputs observed are sourced from upland drainage and deltaic deposits associated with shoreline features of Glacial Lake Duluth or earlier in age. Hobbs & Breckenridge (2011) mapped similar deposits in the Duluth area at approximately the same elevation (1180 feet AMSL) and hypothesized the coarse-grained features were deposited by meltwater streams that flowed at the edge of the Superior lobe as it retreated, prior to the formation of Glacial Lake Duluth. MPCA watershed assessment data (year 2011) indicate good thermal conditions and high brook trout densities (95th

percentile in greater Arrowhead region, Northeast Minnesota) for location SW13 which further supports our conclusions of groundwater upwelling.

For waters with signatures indicative of non-equilibrium evaporation effects, placement of points along the LEL is proportionate to fraction water loss. The LEL is developed using seven sample points that represent baseflow conditions during the severe drought of September 2012. Although the evaporative loss model (Gibson, 2002 & Gibson and Reid, 2010) was developed for open surface waters, it was used to approximate quantitative differences (Fig. 10) between stream watershed locations in this study. Surface waters from stream station SW24 and an upland remnant channel SWR show debatable evaporative losses (7% and 6%) with placement just outside of the error range (2σ) of the LMWL. Compared to all isotope collection sites, a disproportionately large loss (48%) is observed in the Amity Creek headwater wetland (SW10) with wetland regime classification "permanently flooded". This is six times greater than the loss (8%) observed in the East Branch Amity Creek headwater wetland (SW17) with wetland regime classification "saturated". Although clarification could be added through further wetland investigation, it is probable that the increased evaporation in the Amity headwaters (SW10) reflects the permanently flooded state of the wetland regime, whereas water in a saturated wetland (SW17) is primarily held in the substrate as opposed to the land surface therefore decreasing evaporative processes through limited exposure to the atmosphere.

With no signal change observed in the middle to lower reaches of East Branch Amity Creek, the data suggest that main stem Amity Creek has a more complex baseflow

water budget. The second highest tier (11 – 16% loss) in the evaporative loss analysis (Fig. 10) includes Amity Creek sites SW3 and SW22. The latter can be explained by shallower depth to bedrock, lesser overall relief, and wider open channels near the lowest reaches of the system. These physical features can limit groundwater upwelling through inadequate subsurface storage and upland drainage, and increase effective evaporation through lack of overhead cover and advection of heat from the dry warm bedrock surfaces. The former site, located in the mid-watershed is more ambiguous particularly because the groundwater signal at SW11 is located just 1.5 miles upstream. Field observations during sample collection characterize the reach as having isolated and stranded pool habitats interconnected by riffles exhibiting interstitial stream flow. Between stations SW11 and SW3, the Northland sill bounds the stream to the south and negligible wetlands are present. Subsurface storage capacity and groundwater inputs from outside of the hyporheic zone are likely limited in this reach. Along with the East Branch headwater wetland (SW17), site SW1 falls within tier 3 (10-11% loss). Downstream of site SW3 on main stem Amity Creek, fraction water loss initially decreases at site SW24 and is likely due to the mixed flows of East Branch Amity and Amity Creek waters. As expected from increased bedrock influence with longitudinal downstream distance, the water loss to evaporation gradually increases between site SW24 and the mouth of Amity Creek.

The intersection of the LMWL and the LEL ($\delta^{18}O$ = -10.83‰) provides an estimate of the isotopic composition (δ_I) of inflow waters prior to surficial mixing and exposure to evaporative processes. With no lakes or substantially deep aquifers in the

Amity watershed, inflow to individual stream stations is assumed to be shallow-groundwater driven, generally uniform throughout the system, and approximately equal to the weighted mean isotopic composition (δ_P) of annual precipitation. Isotope signatures of baseflow samples collected in 2010 and 2014 on East Branch Amity Creek support the assumption that the typical groundwater signal, prior to effects from evaporative processes or mixing, falls at the intersection of the LMWL and LEL (Fig. 17). East Branch Amity baseflow signatures from sites SW17 ($\delta^{18}O$ = -11.02‰) in 2010 and SW13 ($\delta^{18}O$ = -10.96‰) in 2014 are within the analytical uncertainties of lab analysis from the inflow value. Surface water sample SW12 in 2010 is within the analytical uncertainty for $\delta^{18}O$, but marginally outside of the uncertainty for δD. This may be the result of mixing of lateral inputs into the stronger longitudinal source water during the leaf-off season. By November, less groundwater uptake from trees is occurring in the depressional zone which may result in more storage availability and lateral movement of groundwater to supply stream recharge.

Watershed-Scale Flow Comparison

Percent discharge contribution of East Branch Amity Creek to Amity Creek (Table 2) occurring in study years 2011-2012 was established for varying flow regimes (Fig. 11), identified using records (2002-2012) for the longer-term Amity Creek gage (H02038001). Higher contributions (62-68%) observed in low to mid-range flows are likely due to the strong groundwater inputs that were identified through isotope analysis of baseflow conditions. Annual field observations of late winter to early spring

streamflow on East Branch Amity Creek, while main stem Amity Creek is primarily locked in ice, support the data indicating high baseflow contributions from East Branch Amity Creek. Lower contributions during high and very high flows can be explained by excess storm water inputs and urban runoff to main stem Amity Creek in the lower reaches during high runoff events. Knowing that evaporative losses increase longitudinally downstream from the mid-watershed to the lower reaches, evaporation along with other potential water budget losses (e.g. transpiration and localized loss of streamflow to subsurface flow) within the system during the dry, late summer months may account for lower contributions of East Branch Amity Creek at very low flows.

Reach-Scale Groundwater - Surface Water Interactions

Groundwater Storage Zones.

Two groundwater storage zones within the valley walls of the study reach are defined: near-bank groundwater (NBGW) and depressional groundwater (DGW). Five monitoring wells are defined as NBGW and four as DGW through depth to water duration curve analysis. Near-bank groundwater (bank storage) has frequent interaction with the stream, particularly during event flow, when water moves from the stream into the banks and then returns to the channel as stream levels recede. Location of NBGW wells defines this zone within the boundary of the active floodplain (Fig.13). The maximum width of this zone, encompassing both sides of the stream channel, within the well network is 240 feet (Fig. 13).

The DGW zone has less frequent interaction with the stream, but provides a slow release of storage during periods of low flow. DGW storage is recharged through snowmelt, rain runoff, and above bankfull conditions. The DGW zone is found between the active floodplain boundary of East Branch Amity Creek and the valley walls. Remnant channels, located in this zone, assist in holding water on the landscape for slow infiltration to the shallow groundwater.

Artesian conditions observed in well records (Table 3) indicates groundwater storage capacity exceedance of the shallow aquifer. High frequency and duration of artesian conditions within the NBGW zone indicate limited subsurface storage. Less frequent occurrence at wells (11+00, 13+00, 15+00) located above the high bank of the remnant channel suggest increased capacity in the DGW zone, although still limited with multiple occurrences in a three year period. Artesian conditions within the banks of the remnant channel (mw 14+00) show frequency and duration similar to the near bank zone and represent saturated bed conditions and possibly surficial water storage within the channel.

Groundwater Flow Regimes.

Groundwater exchange relationships with the stream and between the two storage zones in year 2011 can be explained through interpretation of four groundwater flow regimes. Flow regimes are developed through comparison of zone duration curves (Fig. 12). Near-bank groundwater and stream water levels have similar hydrographs (Fig. 14) and are considered equal in this analysis. Flow regime 1 represents very high flow

conditions in which the stream is losing water to the stream banks. During this time, the hydraulic head is higher in NBGW than DGW resulting in an outward subsurface flux. In instances where stream water tops the banks, additional recharge to DGW can occur through infiltration following overland flow. Regime 1 occurs four times in 2011 and accounts for 2% of the time in the 2011 record. The system is in this state for approximately two days following each major runoff event, as observed in April, June, and August 2011 rain response peaks, before entering flow regime 2. April and May 2012 hydrograph peaks likewise show a two-day duration associated with flow regime 1. The system is in this state for an extended six-day period following the June 2012 flood.

The stream transitions to a gaining reach at the start of flow regime 2, when event flow returns to the stream from the banks. During this regime, the subsurface flux reverses as the hydraulic head in the depressional zone stays relatively constant at a higher level and the levels in bank storage rapidly decrease as water moves back into the stream. Delayed melting of snow under a forested canopy, slow infiltration of pooled water on the land surface, and additional upland drainage are plausible sources of continued inputs sustaining DGW while in this regime. Based on 2011 data, this occurs for a period two days to two weeks following the initial response to a major mid- to late-summer rain event and can last as long as six weeks during the spring to early summer season in an average snowpack year (Fig.15b). Sustained time in this regime is also observed (Fig. 15c) in spring of 2012, a low snowpack year.

Flow regime 3 is observed in the dry summer to fall seasons as groundwater continues to discharge to the stream during periods of limited rainfall. During this

regime, the hydraulic head in the DGW zone decreases as storage is released to stream discharge and vegetative uptake. As the NBGW head remains relatively unchanged at stream baseflow levels, the two zones approach equilibrium. In 2011, this occurs for a three week period in June and a three week period in August to September. In June of 2012, the system was in this state for approximately one week prior to the flood. Equilibrium is nearly reached in flow regime 4, when levels in both zones stay relatively constant with time. Hydraulic head may be slightly higher in the DGW zone than the NBGW zone, indicating some lateral movement of subsurface storage to the stream may occur, but longitudinal inputs likely contribute the majority of streamflow during this time. The system was in this state during the dry late-summer to early-fall season of 2011, from mid-September until the loggers were removed prior to ice-up in mid-November, and accounted for 24% of the time in the 2011 record.

Longitudinal and Lateral Inputs.

A strong groundwater signal is recognized through isotope analysis and watershed-scale flow comparison at the study reach during baseflow conditions. Longitudinal and lateral inputs to stream discharge are analyzed and compared over varying climatic conditions. A strong correlation between the isotopic composition of water in the study reach (SW12) and upstream sources (SW17 & SW13) is recognized (Figs. 17 and 18b) during all monitoring conditions, but the tightest relationship is observed during baseflow conditions. Near-bank groundwater (lateral inputs) and stream water hold the same signal following the May 2012 rain event, but compositions differ

slightly during baseflow. Groundwater level data (Fig. 15c) show that the stream is in a losing state, flow regime 1, for days prior to the May 2012 sample collection. Stream conditions reverse to a gaining state, flow regime 2, only one day prior to sample collection which explains the common signal observed between the stream and NBGW rain event samples. Longitudinal upstream signals are most similar to reach composition in baseflow samples which further supports that source waters to stream discharge at the study reach are coming from upstream during baseflow conditions.

Lateral relationships are more complex as observed through comparison of isotopic signatures of stream water to remnant channel, near-bank groundwater, and depressional groundwater (Figs. 17 & 18). Depressional groundwater samples in March and May of 2012 are buffered from surface water signals during snowmelt and rain events. Uniquely, DGW data plot near the theoretical inflow value at the intersection of the LMWL and LEL during runoff events. The DGW compositions are skewed slightly toward winter precipitation which infers that more snowmelt water is mixed into this zone in the spring to early summer season. Surface water composition in the remnant channel suggests equal runoff response to snowmelt as the stream channel. However, the remnant channel is more buffered from runoff during the 3-inch May rain event, showing less compositional influence from precipitation than the stream. This can be explained through canopy interception of rainfall and increased understory vegetation to slow runoff during the growing season. In addition, snowpack depth and water content in the shaded forested portion of the valley may actually be greater during snowmelt due to fewer occurrences of discrete early season thaw events that typically occur January

through early March in areas of high sun exposure. A difference in signals between surface water in the remnant channel and the subsurface DGW zone in both snowmelt and rain runoff events infers either slow infiltration into the bed of the remnant channel or a well-mixed storage zone that is less affected by individual events.

Isotope data results suggest that longitudinal inputs appear to be dominant over lateral inputs at the reach-scale. Water level and isotope data show that lateral inputs increase following runoff events. However, longitudinal inputs likely increase even more during this period. Effective longitudinal inputs may be a function of increased upstream storage in wetlands and groundwater aquifers. In addition, we recognize that the remnant channel historically flowed to Amity Creek. Therefore, riparian storage may flow directionally south to main stem Amity Creek in addition to or in lieu of lateral discharge to the study reach. This would further explain why lateral inputs, as compared to longitudinal, appears to be less of a contributor to baseflow in the study reach of East Branch Amity Creek.

Flood-Induced Changes: Composition, Levels, and Exchange Relationships.

On June 19, 2012, the area was hit by a 500-year flood event, causing major infrastructure damage in Duluth, MN, and eliciting dramatic geomorphic change in reaches of area streams. Geomorphic changes to East Branch Amity Creek included areas of mass slumping in addition to channel incision, thalweg repositioning, and scouring of the remnant channel in the study reach. A flood-induced increase in gradient at an existing stream knick-point was the result of downstream incision and upstream

aggradation at an inactive beaver dam. Downstream incision of approximately 2 vertical feet was estimated based on field observations. At the upstream end of the slope break, an overflow channel connecting the stream to the remnant channel was further eroded as stream water was forced out of the channel at a major bend. Physical changes in the remnant channel included scouring of organics and till, meandering near the low reaches of the well network and addition of new or exposure of existing alluvial fill.

Changes in source water composition and groundwater storage are observed in our data following this event with the most obvious change being a drop in the water table. Because the area was in a state of severe drought by September of 2012, a decrease in groundwater levels from previous years is reasonable. The magnitude of change in the shallow water table, however, was not uniform throughout the well network. Stark decreases in minimum levels (Table 4) from previous years occurred in areas of incision only, including the depressional groundwater storage zone along the remnant channel and the near-bank zone located down gradient of the stream knick-point. This is observed in both 2012 and 2013 data. This relationship between channel incision and lowering of the water table has been documented in other studies. Noel (2009) suggests channel incision can rapidly lower water table elevations for large distances in an adjacent aquifer, potentially modifying the hydrology to a degree capable of influencing adjacent surface-water features. An explanation of this relationship as observed in an Iowa study, Schilling et al. (2004), concludes that channel incision leads to an increase in the hydraulic gradient from high recharge areas to the stream and

encourages groundwater drainage from the riparian zone. In our study, a depleted water table showed no significant signs of rebound one year after the flood.

In addition to channel incision and a decrease in the water table, a change is observed in the isotopic composition of stream baseflow, upstream groundwater inputs, and groundwater storage in the adjacent riparian area. The stream water signature at the study reach is displaced with non-evaporative enrichment from 2010 baseflow signatures, near the theoretical weighted mean annual precipitation value (δ_I), three months after the flood event. The post-flood groundwater signal of the depressional zone changes from a constant pre-flood value of slight depletion from δ_I to a value 0.7 ‰ more enriched than stream water and 1.4 ‰ more enriched than δ_I. The composition of water in the depressional zone is no longer isolated as it has the same post-flood signal as that observed in the near-bank storage zone. This implies that the groundwater in the adjacent storage zones has been replaced or re-mixed through inundation of flood waters. Although stream water shows a more enriched baseflow signal than non-flood years, it shows less enrichment than the surrounding shallow aquifer. This difference in signals is further evidence that the major source of discharge to the study reach during baseflow conditions is upstream groundwater inputs. The data suggest that the upstream source is located near station SW13. This less-enriched stream signal may indicate that the storage zone at SW13 has not been completely replaced by flood waters. We believe this is due to a deeper storage zone at this site and is likely related to the deltaic sediments located there. We observe through the sampling of station SW13 in 2014 that the composition of

the aquifer has returned to its pre-flood composition at the value of weighted mean annual precipitation within two years of the major flood event.

CONCLUSIONS

We conclude that combined stable isotope analysis of Oxygen-18 and deuterium and water table level analysis are useful tools in understanding in detail the hydrology of the Amity Creek system. Isotopic characterization of regional precipitation plays a critical role in explaining groundwater - surface water dynamics in this system and is accomplished through development of a local meteoric water line and local evaporative line for Duluth, MN. The isotopic value for weighted mean annual precipitation is estimated at the intersection of these lines and is assumed to be approximately equal to system inflow. Stream baseflow isotope signatures collected in non-flood years support this assumption. Our data also revealed the potential for using isotopes to identify "lake-effect" precipitation along the North Shore of Lake Superior.

Water budget characterization through evaluation of evaporative and non-evaporative isotopic signals assisted in identifying areas of strong groundwater upwelling in the greater Amity Creek watershed. Deltaic sediment features are located in the vicinity of mid-watershed upwelling areas and are believed to provide enhanced storage of groundwater and subsurface inputs to stream discharge. Isotopic data suggest that longitudinal flow inputs originating from such seeps are more influential than lateral inputs to the downstream study reach and are critical sources of baseflow during dry periods. We hope these areas will be considered for future protection and restoration efforts.

Through depth to water duration curve analysis of well data, two riparian storage zones are identified in the study reach of East Branch Amity Creek. A near-bank zone is located adjacent to the stream, within the active floodplain. Isotope data and time series analysis of water levels show frequent interaction between the stream and this zone, particularly during periods of event flow. Less flashy hydrology is observed in the depressional zone than the near-bank zone with levels remaining sustained at higher elevations for the majority of the year. Four groundwater interaction flow regimes are identified through duration curve comparison and are used to explain the hydrologic interactions between the stream and the surrounding water table and how these relationships vary with change in climatic conditions.

The flood of 2012 altered the area hydrology by lowering the water table and altering the source water composition. We observe a relationship between flood-induced channel incision and lowering of the water table. Incision occurs in both the stream channel and remnant channels located in the flood-prone area within the valley. Isotope analysis shows a change in isotopic composition of groundwater and stream water following the flood. A stable source water composition that is slightly skewed towards winter precipitation from weighted mean annual precipitation is seen in the depressional zone during pre-flood sampling. Water from the stream and the adjacent water table show isotopic enrichment following the flood and is likely due to re-mixing or replacement by flood waters. More enrichment is observed in the depressional groundwater zone than the stream. We believe this is because the aquifer providing strong upwelling at upstream stream reaches is deeper and more buffered from re-mixing

of flood waters. Stream composition returns to the inflow value observed in pre-flood data just two years after the flood. Groundwater levels remained lower one year following the flood.

BIBLIOGRAPHY

Axler, R., Brady, V., Ruzycki, E., Henneck, J., Will, N., Crouse, A., Dumke, J., and Hell, R., 2013. Amity restoration assessment: Water quality, fish, bugs and people. NRRI Technical Report NRRI/TR-2013/29. Natural Resources Research Institute, U. of Minnesota-Duluth, Duluth, MN 55811, 57 p.

Baxter, C. V. and Hauer, F.R., 2000. Geomorphology, hyporheic exchange, and selection of spawning habitat by bull trout (Salvelinus confluentus). Can.J.Fish.Aquat.Sci., 57(7): 1470-1481.

Breckenridge, A., 2013. An analysis of the late glacial lake levels within the western Lake Superior basin based on digital elevation models. Quaternary Research, 80: 383-395.

Carline, R. F., and Brynildson, O.M., 1977. Effects of hydraulic dredging on the ecology of native trout populations in Wisconsin spring ponds. Dept. Nat. Resource. Madison, WI. Tech. Bull. 98, 40 p.

Clark, I. D., and Fritz P., 1997. Environmental Isotopes in Hydrogeology, CRC Press/Lewis Publishers, Boca Raton, FL, 328 p.

Craig, H., 1961. Standard for reporting concentrations of deuterium and oxygen-18 in natural waters. Science, 133: 1833-1834.

Dadaser-Celik, F. and Stefan, H.G., 2008. Lake evaporation response to climate in Minnesota, Project Report Number 506. University of Minnesota St. Anthony Falls Laboratory. Prepared for the Legislative Citizens Committee on Minnesota Resource,. 65 p.

Dansgaard, W., 1964. Stable isotopes in precipitation. Tellus, 16: 436-468.

Farrand, W. R., 1969. The Quaternary history of Lake Superior. In: *Proceedings of the 12th Conference on Great Lakes Research*, pp. 181-197.

Fetter, C.W., 2001. Chapter 2: Elements of the hydrologic cycle. In: *Applied Hydrogeology (4th edn).* Prentice Hall, Upper Saddle River, New Jersey, pp. 24-65.

Fitzpatrick F.A., Peppler M.C., DePhilip M.M. and Lee K.E., 2006. Geomorphic characteristics and classification of Duluth-area streams, Minnesota. USGS Scientific Investigations Report 2006-5029, 54 p.

Fritz, P., Drimmie, R.J., Frape, S.K. and O'Shea, O., 1987. The isotopic composition of precipitation and groundwater in Canada, In: *Isotope Techniques in Water Resources Development*, IAEA Symposium 299, March 1987, Vienna, pp. 539-550.

Froehlich, K., J.J. Gibson and P.K. Aggarwal., 2002. "Deuterium excess in precipitation and its climatological significance." In: *Study of environmental change using isotope techniques*, Vienna, International Atomic Energy Agency, pp. 54–65.

Gammons C.H., Poulson S.R., Pellicori D.A., Reed P.J., Roesler A.J., and Petrescu, E.M., 2006. The hydrogen and oxygen isotopic composition of precipitation, evaporated mine water, and river water in Montana, USA. Journal of Hydrology, 328: 319-330.

Gat, J.R., 1981. Properties of the isotopic species of water: the "isotope effect". In: *Stable Isotope Hydrology, Deuterium and Oxygen-18 in the Water Cycle.* (eds. Gat, J.Rl, Gonfiantini, R.) IAEA Tech. Rep. Ser. No. 210. Int. At. Energy Agency, Vienna, pp. 7-19.

Gat, J.R, and Levy Y., 1978. Isotope hydrology of inland sabkhas in the Bardawil area, Sinai. Limnology and Oceanography, 23: 841-850.

Gibson, J.J., Edwards T.W.D., and Bursey, G.G., 1993. Estimating evaporation using stable isotopes: quantitative results and sensitivity analysis for two catchments in northern Canada. Nordic Hydrology, 24: 79-94.

Gibson, J.J., Prepas, E.E., and McEachern, P., 2002. Quantitative comparison of lake throughflow, residency, and catchment runoff using stable isotopes: modelling and results from a regional survey of boreal lakes. Journal of Hydrology, 262: 128-144.

Gibson, J.J. and Reid, R., 2010. Stable isotope fingerprint of open-water evaporation losses and effective drainage area fluctuations in a subarctic shield watershed. Journal of Hydrology, 381: 142-150.

Golden Gate Weather Services (GGWS). 2015. Minnesota Climate Normals (1981-2010) from National Climatic Data Center [Data file]. Retrieved from http://ggweather.com/normals/MN.html#D

Gonfiantini, R., 1986. Environmental isotopes in lake studies. In: *Fritz, P. (Ed.), Handbook of environmental Isotope Geochemistry, 2: The Terrestrial Environment.* B. Elsevier, Amsterdam, pp. 113-163.

Green, J.C., 1972, North Shore Volcanic Group. In: *Geology of Minnesota: A Centennial Volume*. Sims P. K., and Morey G. B (authors). Minnesota Geological Survey, pp. 294-332.

Harvey, F.E. and Welker, J.M., 2000. Stable isotopic composition of precipitation in the semi-arid north central portion of the US Great Plains. Journal of Hydrology, 238: 90-109.

Hobbs, H.C. and Breckenridge, A., 2011. Ice advances and retreats, inlets and outlets, sediments and strandlines of the western Lake Superior basin. Geological Society of America - Field Guides, 24: 299-315.

Lorenz, D.L., Sanocki, C.A., and Kocian, M.J., 2010. Techniques for estimating the magnitude and frequency of peak flows on small streams in Minnesota based on data through water year 2005: U.S. Geological Survey Scientific Investigations Report 2009–5250, 54 p.

Machavaram W. V. and Krishnamurthy R.V., 1995. Earth surface evaporative process: A case study from the Great Lakes region of the United States based on deuterium excess in precipitation. Geochimica et Cosmochimica Acta, Vol. 59, No. 20, pp. 4279-4283.

Magner, J. A., Regan, C.P, and Trojan, M., 2001. Isotopic Characterization of the Buffalo River Watershed and the Buffalo Aquifer near Moorhead Municipal Well One. Hydrologic Science & Technology, 17: 237-45.

Majoube, M., 1971. Fractionnement en oxygene-18 et en deuterium entre l'eau et sa vapeur. Journal of Chemical Physics, 197: 1423-1436.

Minnesota Climatology Working Group (NCWG), 2010-2013, Minnesota State Climatology Office - DNR Division of Ecological and Water Resources. Daily National Weather Service Temperature, Precipitation, Snowfall, and Snow Depth Data. Station: DULUTH NWS. [Data file]. Retrieved from: http://www.dnr.state.mn.us/climate/historical/acis_stn_meta.html

Minnesota DNR (MNDNR) Section of Fisheries, 2002. unpublished data: trout densities in Amity Creek, St. Louis Co., MN, pp. 1974-2002.

Minnesota Pollution Control Agency (MPCA), 2010-2012. Flow gage data and Year End Summaries for stations H02038001 and H02037005. [Data file].

Minnesota Pollution Control Agency (MPCA), 2014. Lake Superior –South Watershed Monitoring and Assessment Report, 122 p. https://www.pca.state.mn.us/sites/default/files/wq-ws3-04010102b.pdf

Minnesota Pollution Control Agency (MPCA), 2015. Jeffrey Jasperson, personal communication.

Neal, Edward G., 2009. Channel incision and water-table decline along a recently formed proglacial stream, Mendenhall Valley, southeastern Alaska, In: *Studies by the U.S. Geological Survey in Alaska*, Haeussler, P.J., and Galloway, J.P., 2007: U.S. Geological Survey Professional Paper 1760-E, 15 p.

Raleigh, R.F., 1982. Habitat Suitability Index Models: Brook Trout: U.S. Fish Wildl. Serv. FWS/OBS-82/10.24, 42 p.

Rozanski, K., Araguas-Araguas, L, and Gonfiantini, R., 1993. Isotopic patterns in modern global precipitation. In: *Climate change in continental isotopic records,* Am. Geophys. Union, Geophys. Monogr., 78: 1-36.

Rozanski, K., Froehlich, K., Mook, W.G., 2001 Surface water, Vol. III In: *Environmental Isotopes in the Hydrological Cycle: Principles and Applications.* (ed. W.G. Mook). IHP-V, Technical Documents in Hydrology No. 39, UNESCO, Paris, 2001, 117 p.

Schilling, K.E., Zhang, Y.K., and Drobney, P., 2004. Water table fluctuations near an incised stream, Walnut Creek, Iowa. Journal of Hydrology, 286: 236–248

Schultz, N. M., Griffis, T. J., Lee, X. and Baker, J. M., 2011. Identification and correction of spectral contamination in $^{2}H/^{1}H$ and $^{18}O/^{16}O$ measured in leaf, stem, and soil water. Rapid Commun. Mass Spectrom., 25: 3360–3368.

Siergieiev, D., Ehlert, L., Reimann, T., Lundberg, A., and Liedl, R., 2015. Modelling hyporheic processes for regulated rivers under transient hydrological and hydrogeological conditions. Hydrol. Earth Syst. Sci., 19: 329-340.

Sims P. K., and Morey G. B., 1972. Geology of Minnesota: A Centennial Volume. Minnesota Geological Survey. 632 p.

Sklash, M. G. and Farvolden, R. N., 1982. The use of environmental isotopes in the study of high-runoff episodes in streams. In: *Isotope Studies of Hydrologic*

Processes (eds. E. C. Perry, Jr. and C. W. Montgomery). Northern Illinois University Press. DeKalb, Illinois pp. 65-73.

Ward, A.D., and Elliot, W.J., (1995) Environmental Hydrology. Boca Raton, FL: CRC Press, 462 p.

Webster, D., and Eiriksdotteir. 1976. Upwelling water as a factor influencing choice of spawning sites by brook trout (*Salvelinus fontinalis*). Trans. Am. Fish. Soc. 75: 257-266.

Wick, M., 2013. Identifying Erosional Hotspots in Streams Along the North Shore of Lake Superior, Minnesota using High-Resolution Elevation and Soils Data. M.S. Thesis, University of Minnesota. 91 p.

Winter, T. C., Harvey, J.W., Franke, O. L., and Alley, W. M., 1998. The Hydrologic Cycle and Interactions of Ground Water and Surface Water In: *Ground Water and Surface Water: A Single Resource*. USGS Circular 1139. pp. 2-20.

APPENDIX 1. STABLE ISOTOPE LAB ANALYSIS RESULTS: AMITY CREEK WATERSHED, DULUTH, MN

Table A1: Lab results for $\delta^{18}O$ and $\delta^{2}H$ and atmospheric conditions as reported from the Duluth International Airport weather station, United States.(Lat: 46.84N, Lon: 92.23W).

Sample Station	**Sample Type**	**Event Type**	**Calendar Date**	**$\delta^{2}H$** (‰)	**$\delta^{18}O$** (‰)	Max/Mean Daily **Temperature** (°C)	Max/Mean Daily **Humidity** (%)
mw13+00	DGW	snowmelt	2012/03/20	-79.22	-11.51	-	-
mw15+00	DGW	rain event	2012/05/30	-79.39	-11.32	-	-
mw11+00	DGW	baseflow	2012/09/14	-63.80	-9.42	-	-
mw4+00	NBGW	baseflow	2010/11/17	-69.29	-9.87	-	-
mw4+00	NBGW	rain event	2012/05/30	-53.69	-7.77	-	-
mw4+00	NBGW	baseflow	2012/09/14	-65.53	-9.60	-	-
SW_R	SWR	snowmelt	2012/03/20	-91.16	-12.72	-	-
SW_R	SWR	rain event	2012/05/30	-70.68	-9.99	-	-
SW_R	SWR	baseflow	2012/09/14	-67.10	-9.50	-	-
SW1	SWS	snowmelt	2012/03/20	-93.05	-14.18	-	-
SW1	SWS	rain event	2012/05/24	-47.29	-7.22	-	-
SW1	SWS	baseflow	2012/09/14	-65.86	-9.06	-	-
SW10	SWS	snowmelt	2012/03/20	-92.66	-12.54	-	-
SW10	SWS	rain event	2012/05/24	-48.38	-7.18	-	-
SW10	SWS	baseflow	2012/09/14	-44.36	-5.01	-	-
SW11	SWS	rain event	2012/05/24	-47.81	-7.40	-	-
SW11	SWS	baseflow	2012/09/14	-59.72	-8.87	-	-
SW12	SWS	baseflow	2010/11/17	-77.31	-10.67	-	-
SW12	SWS	snowmelt	2012/03/20	-94.80	-13.14	-	-
SW12	SWS	rain event	2012/05/30	-51.08	-7.76	-	-
SW12	SWS	baseflow	2012/09/14	-67.87	-10.14	-	-
SW13	SWS	snowmelt	2012/03/20	-93.65	-12.70	-	-
SW13	SWS	rain event	2012/05/24	-47.23	-7.17	-	-
SW13	SWS	baseflow	2012/09/14	-67.38	-10.25	-	-
SW13	SWS	baseflow	2014/07/23	-75.76	-10.96	-	-
SW17	SWS	baseflow	2010/11/17	-76.95	-11.02	-	-
SW17	SWS	snowmelt	2011/04/11	-95.56	-13.78	-	-
SW17	SWS	snowmelt	2012/03/20	-92.15	-12.68	-	-
SW17	SWS	rain event	2012/05/24	-46.46	-8.32	-	-
SW17	SWS	baseflow	2012/09/14	-67.77	-9.17	-	-
SW2	SWS	snowmelt	2012/03/20	-95.27	-13.15	-	-
SW22	SWS	snowmelt	2012/03/20	-93.85	-12.60	-	-
SW22	SWS	rain event	2012/05/24	-46.50	-7.14	-	-
SW22	SWS	baseflow	2012/09/14	-63.77	-8.62	-	-
SW24	SWS	snowmelt	2011/04/11	-94.24	-13.82	-	-
SW24	SWS	rain event	2012/05/24	-45.33	-7.11	-	-
SW24	SWS	baseflow	2012/09/14	-66.87	-9.41	-	-
SW3	SWS	baseflow	2010/11/17	-76.09	-10.32	-	-
SW3	SWS	snowmelt	2011/04/11	-92.38	-13.12	-	-
SW3	SWS	snowmelt	2012/03/20	-91.80	-13.34	-	-
SW3	SWS	snowmelt	2012/03/21	-86.17	-12.00	-	-
SW3	SWS	rain event	2012/05/24	-43.75	-8.02	-	-
SW3	SWS	baseflow	2012/09/14	-61.16	-7.95	-	-
SW4	SWS	snowmelt	2012/03/20	-90.20	-12.33	-	-

Sample Station	Sample Type	Event Type	Calendar Date	δ^2H (‰)	$\delta^{18}O$ (‰)	d-excess (%)	Max/Mean Daily Temperature (°C)	Max/Mean Daily Humidity (%)
PRECIP_12	snow	snow	2011/04/11	-95.22	-13.76	14.83	14/10	83/57
PRECIP_17	snow	snow	2011/04/11	-98.48	-13.91	12.83	d	d
PRECIP_22	snow	snow	2011/04/11	-87.12	-11.73	6.71	d	d
PRECIP_8	snow	snow	2011/04/11	-93.03	-13.70	16.60	d	d
PRECIP_1	snow	snow	2012/03/12	-111.96	-15.58	12.68	6/4	100/83
PRECIP_10	snow	snow	2012/03/12	-115.05	-15.91	12.20	d	d
PRECIP_11	snow	snow	2012/03/12	-117.01	-15.89	10.11	d	d
PRECIP_13	snow	snow	2012/03/12	-117.57	-16.30	12.80	d	d
PRECIP_17	snow	snow	2012/03/12	-126.35	-16.99	9.54	d	d
PRECIP_22	snow	snow	2012/03/12	-111.70	-15.42	11.63	d	d
PRECIP_12	snow	snow	2012/03/20	-104.76	-14.10	8.02	16/13	93/83
PRECIP	snow	snow	2012/11/24	-183.65	-23.70	5.95	-7/-12	87/77
PRECIP	rain	rain event	2011/04/11	-62.83	-8.89	8.26	d	d
PRECIP	rain	rain event	2012/04/15	-38.70	-7.91	24.56	11/8	89/76
PRECIP	rain	rain event	2012/05/19	-1.19	-1.73	12.62	27/21	93/69
PRECIP	rain	rain event	2012/05/24	-23.41	-4.44	12.08	15/13	100/92
PRECIP	rain	rain event	2012/06/20	-26.89	-5.24	15.04	22/18	97/88
PRECIP	rain	rain event	2012/08/18	-88.11	-12.11	8.74	24/17	93/69
PRECIP	rain	rain event	2012/09/19	-123.65	-14.54	-7.37	19/13	80/62
PRECIP	rain	rain event	2012/10/25	-82.79	-11.44	8.71	7/3	92/84

DGW = depressional groundwater. **NBGW** = near bank groundwater. S**WR** = surface water, remnant channel.
SWS = surface water, stream. **d** = duplicate information provided for this date at another sample station.
PRECIP taken at Lat: 46.83N, Long:-92.03W. "**PRECIP_value**" taken at the corresponding SWS station.

APPENDIX 2. ISOTOPE MODEL FOR FRACTION WATER LOSS BY EVAPORATION

As explained in Gibson et al. (2002) and Gibson and Reid (2010), the fraction of water loss by evaporation for a well-mixed lake with inflow and open water evaporation can be expressed as

$$\chi_L = \frac{E_L}{I_L} = \left(\frac{\delta_L - \delta_I}{m\ (\delta^* - \delta_L)}\right) \text{ (dimensionless)} \quad (1)$$

where E_L is evaporation (m^3) and I_L is the combined surface and subsurface inflow (m^3) to the open water system. The numerator in the final expression is determined from the isotopic composition in del notation of the evaporating water body, the sample water (δ_L), and inflow water (δ_I), where the inflow water value is determined from the intersection of the LMWL and the LEL. The denominator is determined by the enrichment slope (m) and the limiting isotopic enrichment (δ^*) which is dependent on atmospheric conditions.

$$m = (h - \varepsilon/1000)/(1 - h\ + \varepsilon_k/1000) \quad (2)$$

$$\delta^* = (h\ \delta_A + \varepsilon)/(h - \varepsilon/1000)\ \ (‰) \quad (3)$$

Humidity is normalized to the temperature of the water surface and is dependent on the relative humidity measured in air (h_i) and the saturation vapour pressure (p) with respect to air and water temperature. Normalized relative humidity (h) is expressed as:

$$h = h_i \left(\frac{p_{sat(air)}}{p_{sat(water)}}\right) \quad (4)$$

The saturation vapor pressure is calculated from the empirical equation outlined in Rozanski et al. (2001) and Ward and Elliot (1995):

$$p_{sat(air)} = exp\left(\frac{16.78\,T_{air} - 116.9}{T_{air} + 237.3}\right) \text{[kP]} \quad (5)$$

$$p_{sat(water)} = exp\left(\frac{16.78\,T_{water} - 116.9}{T_{water} + 237.3}\right) \text{[kP]} \quad (6)$$

The limiting isotopic enrichment (Gat and Levy, 1978; Gat, 1981; Gibson and Reid, 2010) is the enrichment value approached by residual water of an evaporating water body and is a function of the total isotopic separation factor (ε) and the isotopic composition of ambient moisture over the water body (δ_A). The isotopic separation includes the equilibrium (ε^*) and kinetic (ε_K) components. The kinetic component is controlled by molecular diffusion at the water-air interface and is a function of the humidity deficit as expressed in Eq. (9) below. The equilibrium component accounts for

the equilibrium of water and air and is a function of water temperature (K) as determined by Majoube (1971) and outlined in Gibson (2010).

$$\varepsilon = \varepsilon^* + \varepsilon_K \quad (‰) \tag{7}$$

$$\varepsilon^* = -7.685 + 6.7123\left(\frac{10^3}{T}\right) - 1.6664(10^6/T^2) + 0.35041(10^9/T^3)\ (‰) \tag{8}$$

$$\varepsilon_K = C_K(1-h)\ \ (‰) \tag{9}$$

where C_K= 14.2 ‰ for oxygen, as derived from laboratory experiments (Gonfiantini, 1986).

$$\delta_A = \delta_P - \varepsilon^* \quad (‰) \tag{10}$$

where δ_P is the mean isotopc compostion of local precipitation. For this study, it is assumed that the main source of water for the stream during dry periods is well-mixed groundwater supplied from a shallow aquifer that represents mean annual precipitation. Based on this assumption, the isotopic composition for precipitation is equivalent to the inflow water (δ_I).

MODEL RESULTS

Table A2-1. Model output of percent water loss to evaporation for Amity Creek watershed surface water sample locations, September 2012.

Station	Description	% Loss to Evaporation
SW10	Amity Creek, headwater wetland	48
SW3	Amity Creek, upstream of E. Br. Amity Creek confluence	16
SW22	Amity Creek, lower reach, bedrock	12
SW1	Amity Creek, top of escarpment, bedrock	9
SW17	E. Br. Amity Creek, headwater wetland	8
SW24	Amity Creek, downstream of E. Br. Amity Creek confluence	7
SWR	Remnant channel	6
SW13	E. Br. Amity Creek, mid-watershed	0
SW12	E. Br. Amity Creek,study reach	0
SW11	Amity Creek, mid-watershed	0